Polymer Journal (2018) 50, 127–147

www.nature.com/pj

REVIEW

Topology-transformable polymers: linear–branched polymer structural transformation via the mechanical linking of polymer chains

Toshikazu Takata and Daisuke Aoki

In this review article, we discuss the synthesis and dynamic nature of macromolecular systems that have mechanically linked polymer chains capable of undergoing a topology transformation driven by a rotaxane molecular switch. The rotaxane linking of polymer chains plays a crucial role in these systems. A linear polymer possessing a crown ether/*sec*-ammonium salt-type [1] rotaxane moiety at the axle chain terminal was prepared via the rotaxane linking of a single polymer chain. A linear–cyclic polymer topology transformation was achieved via the movement of the wheel component from one end to the other end of the axle component using the rotaxane macromolecular switch function. The successful synthesis of a macromolecular [2]rotaxane (M2R) possessing a single polymer axle and one crown ether wheel led to a variety of unique applications, such as the development of topology-transformable polymers and the synthesis of rotaxane crosslinked polymers (RCPs). The introduction of a polymer chain to the wheel component of M2R (rotaxane linking of two polymer chains) produced a rotaxane-linked AB block copolymer that transformed its topology from linear to branched. Furthermore, a rotaxane-linked three-component polymer and an ABC triblock copolymer were synthesized and transformed to the corresponding 3-arm star (co)polymers, and the transformation was confirmed by measuring the hydrodynamic volume change. The structural transformation of 4-arm and 6-arm star polymers was also accomplished using the dynamic mobility of a similar rotaxane. As a useful application, M2R-based vinylic crosslinkers (RCs) were prepared and applied to the synthesis of RCPs, whereby the addition of RCs into radical polymerization systems of vinyl monomers afforded polymers with excellent toughness by enhancing both of tradeoff properties that cannot be achieved using typical covalent crosslinkers.
Polymer Journal (2018) **50,** 127–147; doi:10.1038/pj.2017.60; published online 25 October 2017

INTRODUCTION

The shape or topology of a polymer is one of the most essential factors determining its properties. A variety of polymer structures, such as linear, cyclic, branched and grafted, have been reported so far (Figure 1) along with their structure-dependent properties. The development of simple homopolymers to copolymers, including block copolymers and their associated polymer topologies, would further expand the versatile possibilities in polymer science. For example, compared with linear polymers, corresponding topological polymers,[1–9] such as star polymers,[10,11] cyclic polymers,[12–14] dendrimers[15] and hyperbranched polymers,[16] generally have a smaller hydrodynamic volume and lower viscosity in solution and less polymer entanglement in bulk. These properties are useful in solid materials and can help to not only reduce the amount of solvent to afford sustainable materials but also make the molding process easy because of the low melt viscosity.[17–20] Meanwhile, from the viewpoint of dynamic system construction, the mutual structural transformation of polymers with different topologies is generally impossible because the structures of most polymers are held together by covalent bonds. Although supramolecular polymers are sufficiently structurally soft to change their structures because of the weak intermolecular interaction between the monomer units, their actual use is limited owing to their reduced stability under normal conditions. The realization of structural transformation and/or reversible transformation between such structurally different polymers makes the breadth of polymers infinitely wide and allows the generation of many dynamic polymer systems.

To transform the polymer topology while maintaining sufficient structural stability similar to that of a covalent compound, a dynamic polymer system that undergoes a topological change without cleavage of the covalent bond is required. This system can be accomplished only by using polymer systems that have mechanically linked polymer chains. Dynamic molecular and macromolecular systems driven by the control of mechanical or noncovalent linkages, enabling changes in the polymer topology, are very attractive not only from a scientific perspective but also for actual applications, such as smart devices and materials.[21–31] Among such linkages, rotaxane linkages are the most promising because rotaxane molecules can survive without any interactions between the components, that is, the components display

Department of Chemical Science and Engineering, Tokyo Institute of Technology and JST-CREST, Tokyo, Japan
Correspondence: Professor T Takata, Department of Chemical Science and Engineering, Tokyo Institute of Technology and JST-CREST, 2-12-1 Ookayama, Meguro-ku, Tokyo 152-8552, Japan.
E-mail: takata.t.ab@m.titech.ac.jp
Received 31 July 2017; revised 6 August 2017; accepted 7 August 2017; published online 25 October 2017

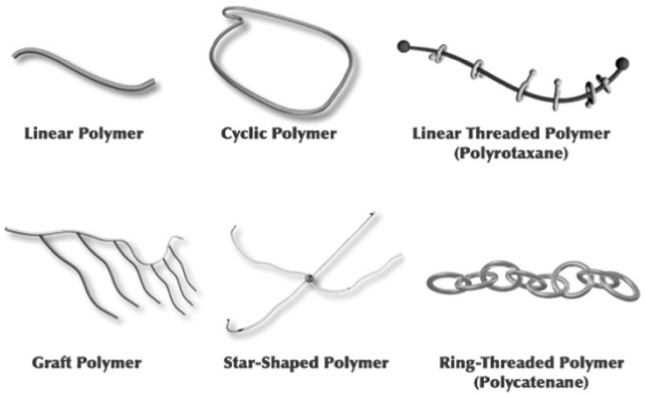

Figure 1 A variety of polymer shapes. A full colour version of this figure is available at the *Polymer Journal* journal online.

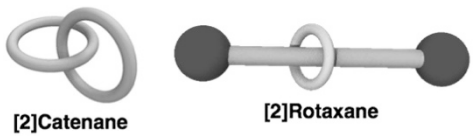

Figure 2 Structures of [2]catenane and [2]rotaxane, as simple mechanically linked molecules. A full colour version of this figure is available at the *Polymer Journal* journal online.

a high degree of freedom and mobility. Therefore, macromolecules consisting of rotaxane-linked polymer units should show dynamic characteristics, for example, topological changes, in addition to unique properties that have not been attained so far. The 2016 Nobel Prize in Chemistry was awarded to researchers, including two rotaxane investigators (Sauvage and Stoddart), for their work on 'molecular machines'. Therefore, the application of molecular machines to sophisticated dynamic systems, such as rotaxane-linked polymers, may be a future target.

Figure 2 shows the schematic structures of the simplest interlocked compounds [2]catenane and [2]rotaxane, whereby their components are movable and have a high degree of freedom because of the mechanical linkage. However, the components are strongly linked; therefore, their separation requires the same amount of energy as a covalent bond, in contrast to supramolecular systems constructed of hydrogen bonds or coordination bonds. In particular, rotaxane structures are highly suitable for linking polymer chains. As rotaxanes have a wheel component capable of walking along the linear axle, the introduction of a polymer chain into these components results in the construction of a mobile system comprising the connected polymer chains.

Matsushita and colleagues[32,33] reported the interesting topology-dependent morphology of two types of three-component polymers with linear and star shapes. As shown in Figure 3, the linear ABC triblock copolymer and star polymer composed of three different polymer chains show unique characteristics, such as microphase-separated structures, owing to their topology.[32,33] It is no wonder that these two polymers with different topologies cannot interconvert unless the covalent bond is broken and rearranged.

Rotaxane-linked polymer systems, however, can solve this problem. As shown in Figure 4, the rotaxane-linked ABC triblock copolymer consisting of a BC diblock copolymer chain and a polymer chain A connected to a rotaxane wheel undergoes a wheel movement along the B polymer chain to afford an initially grafted or branched triblock

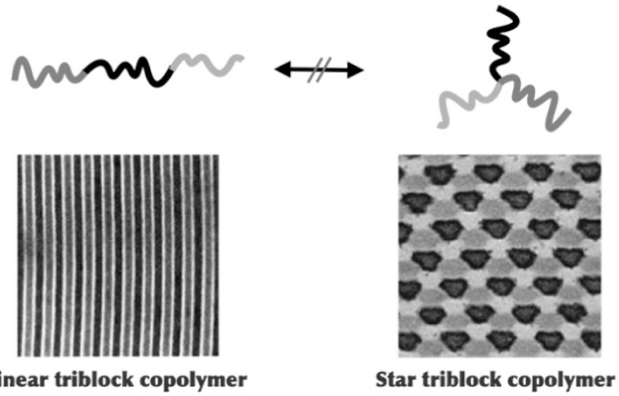

Figure 3 Topology-dependent morphology of two types of three-component polymers with linear and star shapes. Adapted with permission from Mogi *et al.*[32] and Takano *et al.*[33]. Copyright American Chemical Society. A full colour version of this figure is available at the *Polymer Journal* journal online.

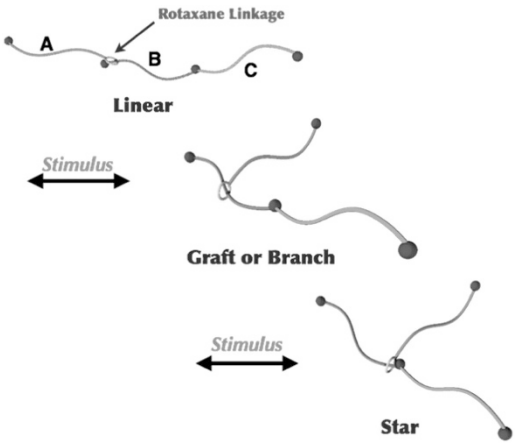

Figure 4 Structural transformation of a linear ABC triblock copolymer containing rotaxane-linked units to graft or branched and star polymers. A full colour version of this figure is available at the *Polymer Journal* journal online.

copolymer and finally an ABC star polymer, depending on the wheel position on the B polymer. Furthermore, the present system is also reversible if the stimuli responsible for the movement of the rotaxane moiety are reversible.

Thus, the rotaxane linking of polymer chains is anticipated to provide many opportunities for constructing a variety of dynamic polymer systems. In this review article, we summarize the synthesis and topology transformation of dynamic polymer systems characterized by rotaxane-linked polymer chains.

BASIS FOR THE MOLECULAR DESIGN OF A TOPOLOGY-TRANSFORMABLE POLYMER

To prepare the abovementioned rotaxane-linked polymer systems, new technology is required in which one wheel component threads a single polymer chain to afford the simplest polyrotaxane, that is, macromolecular [2]rotaxane (M2R). Studies of the synthesis and application of a variety of polyrotaxanes, mainly main-chain-type polyrotaxanes, have so far been directed toward the development of innovative polymer materials by using the dynamic nature of the components rather than the construction of novel polymers. Several comprehensive reviews and books cover these works.[25,28–31] Although many polyrotaxanes have been reported over the past two decades, few

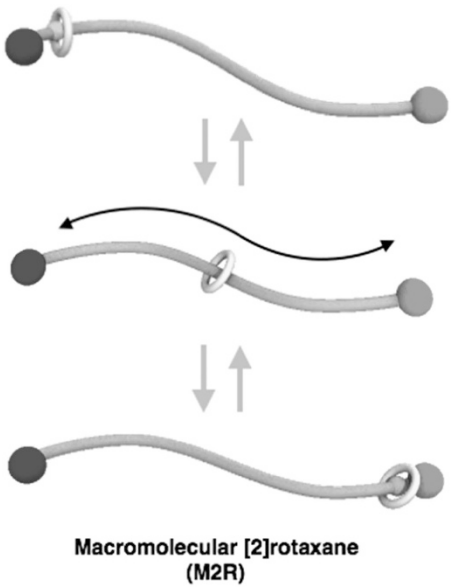

Figure 5 Macromolecular [2]rotaxane (M2R) and a macromolecular switch based on M2R. A full colour version of this figure is available at the *Polymer Journal* journal online.

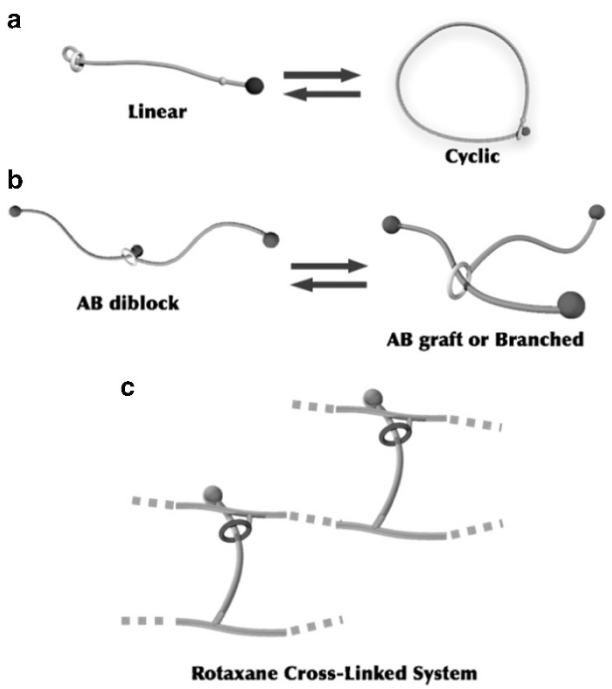

Figure 6 Dynamic macromolecular systems derived from macromolecular [2] rotaxane (M2R). (**a**), (**b**) topology transformation system, (**c**) rotaxane cross-linked system. A full colour version of this figure is available at the *Polymer Journal* journal online.

structure-definite polyrotaxanes have appeared, presumably because of the synthetic difficulty. In particular, the synthesis of M2R was a large challenge until two groups, including us, reported the first controlled synthetic method several years ago.[34,35] In addition to the synthesis of M2R, the development of macromolecular switches (Figure 5) based on the controllable location and mobility of the components is also indispensable for the construction of dynamic polymer systems. M2R endowed with a switching function should have great potential.

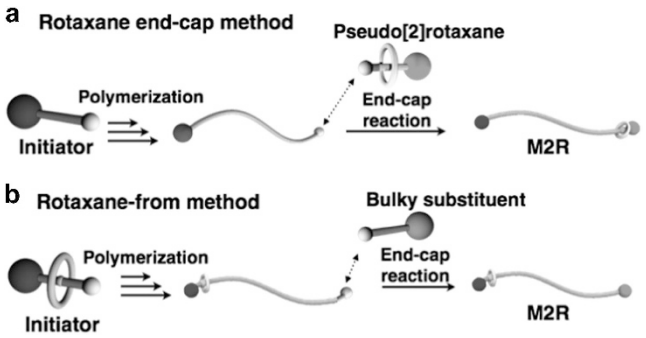

Figure 7 Two synthetic strategies of macromolecular [2]rotaxane (**M2R**) through (**a**) the rotaxane end-cap method and (**b**) the rotaxane-from method. A full colour version of this figure is available at the *Polymer Journal* journal online.

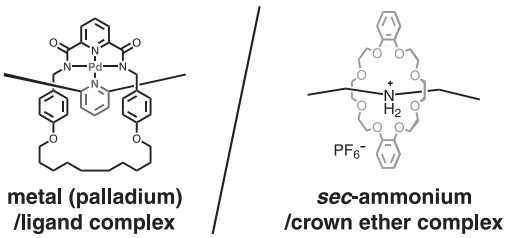

Figure 8 *sec*-Ammonium/crown ether complex and metal (palladium)/ligand complex as couples formed by strong attractive interactions that can be used for the preparation of macromolecular [2]rotaxane (M2R) but can be removed for enhanced mobility. A full colour version of this figure is available at the *Polymer Journal* journal online.

With the achievement of switchable M2R, a variety of dynamic polymer systems, such as those shown in Figures 4 and 6, could be developed. Here, we discuss the synthesis and properties of M2R-based topology-transformable polymer systems as stimuli-responsive polymer systems, mainly focusing on linear–branched topology transformations (Figures 4 and 6) after the basic introduction of linear–cyclic polymer topology transformations. Furthermore, we also briefly discuss rotaxane crosslinked systems that can be regarded as an application of such rotaxane-linked polymer systems (Figure 6).

SYNTHETIC STRATEGY OF M2R

Figure 7 illustrates the synthetic strategies of M2R, in which the wheel component can move from one end to the other end of the axle component assuming the axle is fixed, reported so far.[34,35] The most important point in the synthesis of M2R is to carefully construct the threaded structure between the polymer axle and macrocycle wheel components.

The key step in the rotaxane end-cap method for M2R (Figure 7a) is the connection of a terminal, bulky telechelic polymer as the axle polymer and a pseudo[2]rotaxane as the wheel component. As this key step involves the end-cap reaction of the axle terminal of pseudo[2] rotaxane with the polymer terminal, highly efficient reactions, such as click reactions, are required. Even with the use of a click reaction, excess pseudo[2]rotaxane is usually required to achieve the binding of the two termini. Despite such restriction, this method has merits such as structural diversity of the polymer used for the end-cap reaction, indicating the usefulness of the method.

In contrast, the rotaxane-from method (Figure 7b) uses pseudo[2] rotaxane as an initiator for the living polymerization of a monomer to prepare the axle polymer chain, followed by reaction of the

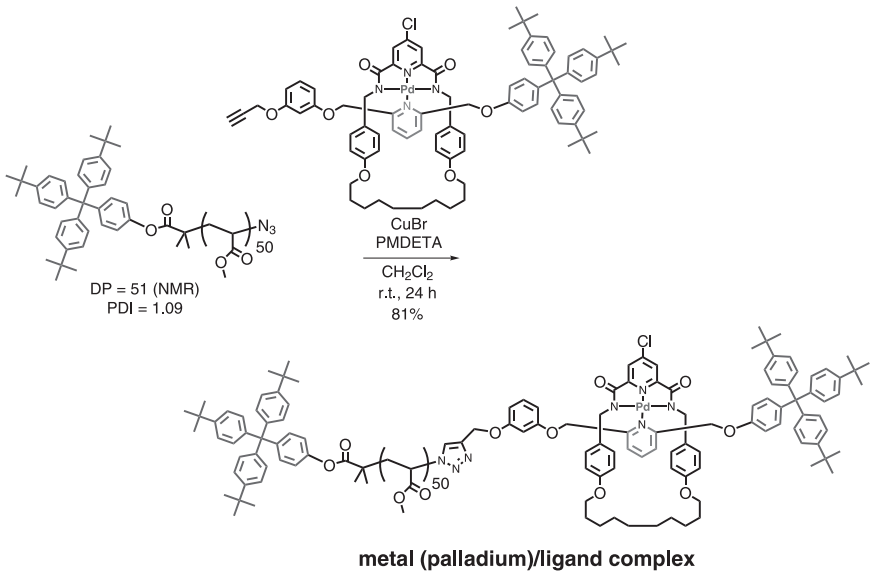

Scheme 1 Synthesis of a palladium (Pd) complex-based macromolecular [2]rotaxane (M2R) via the rotaxane end-cap method. A full colour version of this figure is available at the *Polymer Journal* journal online.

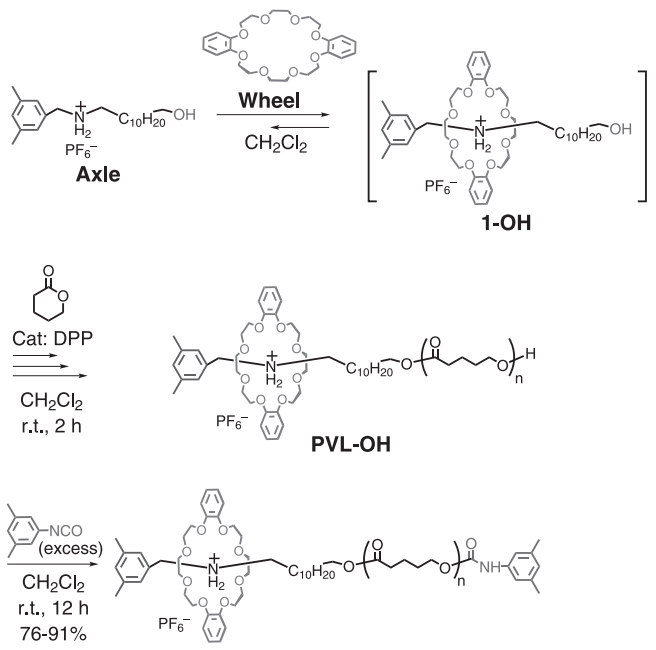

Scheme 2 Synthesis of *sec*-ammonium salt/crown ether-based macromolecular [2]rotaxane (M2R) via the rotaxane-from method. A full colour version of this figure is available at the *Polymer Journal* journal online.

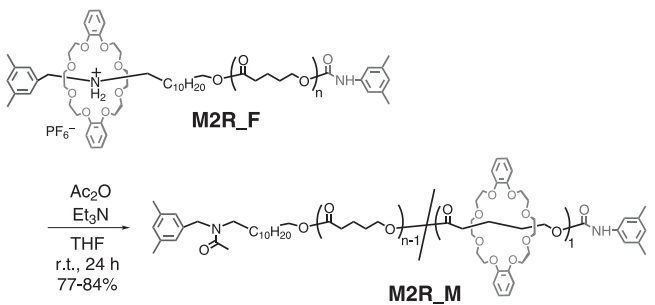

Scheme 3 Synthesis of **M2R_M** with enhanced component mobility by *N*-acetylation of **M2R_F.** M2R, macromolecular [2]rotaxane. A full colour version of this figure is available at the *Polymer Journal* journal online.

propagating end with a bulky end-cap to prevent the deslippage of the wheel component. Notably, excess pseudo[2]rotaxane is not required in this method because one pseudo[2]rotaxane initiator gives one M2R when the initiator efficiency is 100%. Judging from the troublesome purification of M2R during the removal of the polymer agent used in the end-cap reaction in the rotaxane end-cap method, the rotaxane-from method seems superior to the rotaxane end-cap method; impurities, such as excess reagents, monomers and by-products, can be removed by simple precipitation and/or preparative gel permeation chromatography (GPC).

To synthesize dynamic polymer systems based on rotaxane linkages, M2R components should have a relatively position-controllable functionality, such as a macromolecular switch. Namely, strong intercomponent interactions used for the synthetic process of M2R should be removed by some stimulus to convert the structure; as a result, new interactions between the rotaxane-linked components should emerge to switch their relative position. The interaction between a *sec*-ammonium/crown ether complex[36–42] or a metal (palladium)/ligand complex[34,43–49] with M2R components is sufficiently strong to maintain the structures of the components but can be removed by some stimuli to change their relative position (Figure 8). Meanwhile, the design of an M2R consisting of cyclodextrin as a wheel and a polymer as an axle is difficult compared with the above two cases (Figure 8) because the wheel number and the relative position of the components are usually uncontrollable.[23,28]

SYNTHESIS OF M2R

Fustin and colleagues[34] first reported the successful synthesis of M2R and a rotaxane-linked block copolymer (RLBC) using the rotaxane end-cap method. They used a macrocyclic palladium complex with a pseudorotaxane structure as the end-cap agent. The end-cap proceeded efficiently via the Huisgen click reaction with terminal azide-

functionalized poly(methyl acrylate), as shown in Scheme 1. The high isolated yield of the end-cap reaction (81%) can be attributed to the highly efficient Huisgen click reaction and the high stability of the square planar palladium(II) complex. No palladium-free M2R was studied to evaluate the mobility of the M2R components.

The combination of a 24-membered crown ether, such as dibenzo-24-crown-8-ether (DB24C8), and *sec*-ammonium salt has been widely used for rotaxane synthesis.[38,42,50] Takata and colleagues[51–53] developed various *sec*-ammonium salt/DB24C8-based rotaxanes and applied them to rotaxane switches in which the mobility and relative position of the rotaxane components could be controlled. Therefore, M2R possessing the *sec*-ammonium salt/DB24C8 couple can be regarded as an ideal structure-definite polyrotaxane in which the mobility and position of the components should be stimuli responsive.

Takata and colleagues[35] recently developed an effective synthetic protocol of M2R via the rotaxane-from method that produced M2R in high yield with high purity. As discussed above, the rotaxane-from method using pseudo[2]rotaxane as an initiator of living polymerization has the following advantages: (1) the amount of pseudo[2] rotaxane prepared through the relatively complicated processes is minimized, but the [2]rotaxane structure is introduced into all polymer chains, and (2) the purification of the synthesized M2R is easy because M2R and impurities are separated via simple

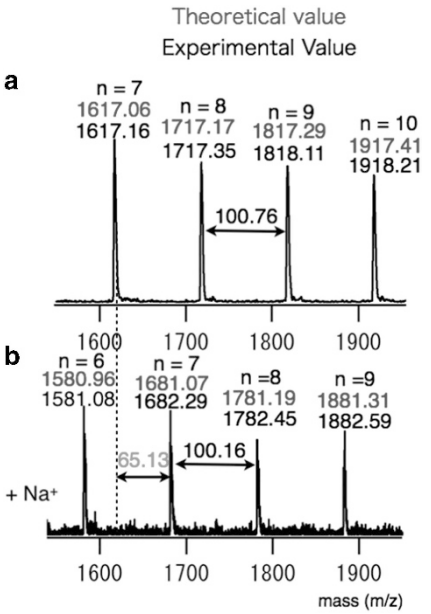

Figure 9 Matrix-assisted laser desorption/ionization time-of-flight mass spectrometry (MALDI-TOF-MS) spectra of (**a**) **M2R_F** and (**b**) **M2R_M**. M2R, macromolecular [2]rotaxane. A full colour version of this figure is available at the *Polymer Journal* journal online.

Table 1 Synthesis[a] and thermal properties of M2Rs with different DPs

Code	*$[M]_0/[I]_0$*	*Yield[b] [%]*	*DP[c]*	T_m[d]	δH_m[e]
M2R10-F	10	86	10	—[f]	—[f]
M2R10-M	—	77	10	—[f]	—[f]
M2R14-F	15	76	14	—[f]	—[f]
M2R14-M	—	80	14	—[f]	—[f]
M2R17-F	20	87	17	42	39
M2R17-M	—	79	17	—[f]	—[f]
M2R33-F	35	79	33	39	59
M2R33-M	—	78	33	32	57
M2R49-F	50	87	49	42	61
M2R49-M	—	77	49	40	60
M2R97-F	100	89	97	44	68
M2R97-M	—	84	97	42	69

Abbreviations: DP, degree of polymerization; M2R, macromolecular [2]rotaxane.
The differential scanning calorimetry (DSC) data were obtained during the second heating at a heating rate of 10 °C per min.
[a]Polymerization conditions: $[I]_0 = 40$ mmol l^{-1}, $[DPP]_0/[I]_0 = 1$, ambient temperature.
[b]Isolated yield by preparative gel permeation chromatography (GPC) eluted with $CHCl_3$.
[c]Degree of polymerization determined by ^1H nuclear magnetic resonance (NMR).
[d]Melting temperature.
[e]Melting enthalpy.
[f]Not observed.

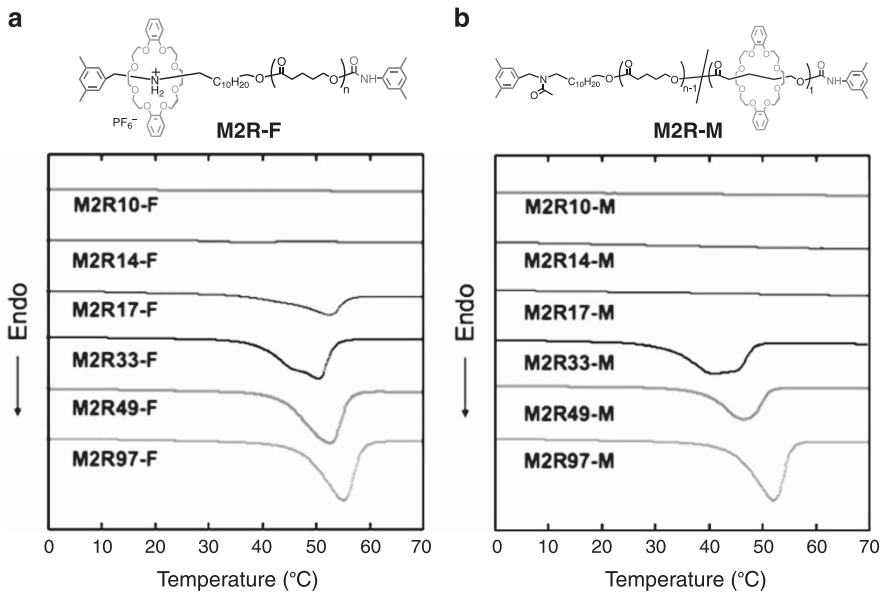

Figure 10 Differential scanning calorimetry (DSC) heating curves of (**a**) **M2R-F**s and (**b**) **M2R-M**s with different degrees of polymerization (DPs; second heating) at a heating rate of 10 °C per min. M2R, macromolecular [2]rotaxane. A full colour version of this figure is available at the *Polymer Journal* journal online.

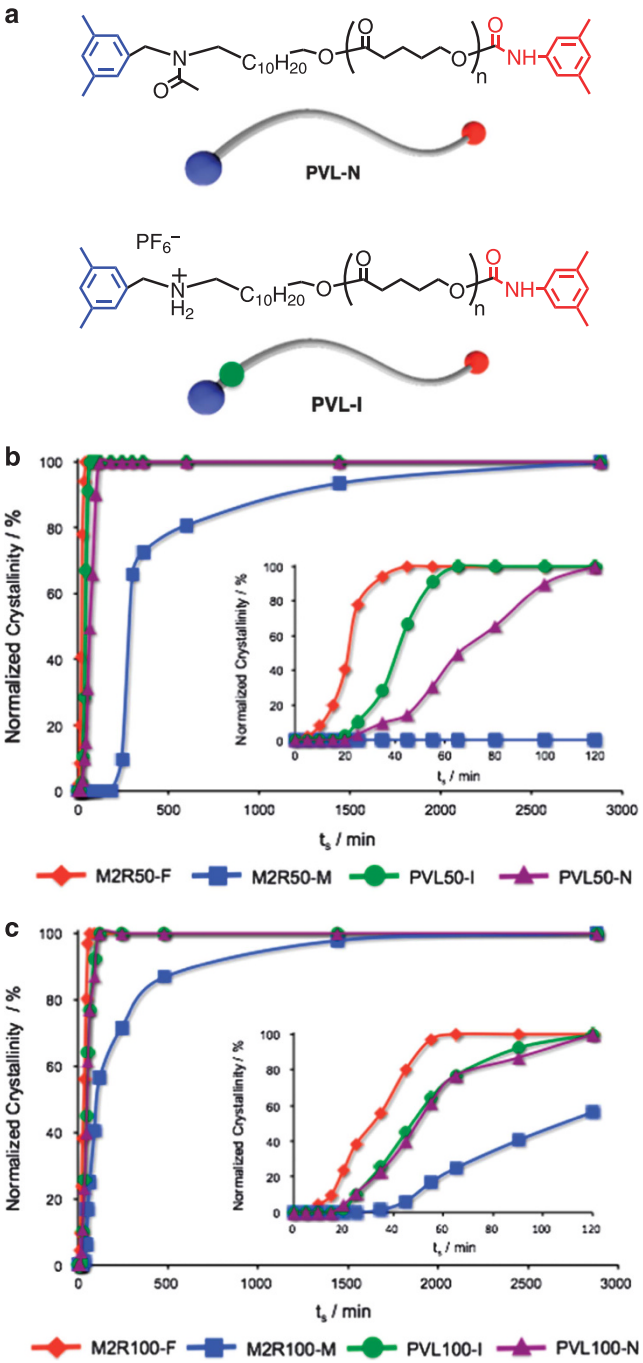

Figure 11 Time-dependent crystallinity of **M2R**s. (**a**) Structures of **PVL-I** and **PVL-N**. Crystallinity measured by differential scanning calorimetry (DSC) at a constant temperature (T_{sc}): (**b**) at 34 °C for degree of polymerization (DP) = 50 PVL and (**c**) at 38 °C for DP = 100 PVL (100% crystallinity = melting enthalpy obtained by nonisothermal measurement with a heating rate of 10 °C per min). M2R, macromolecular [2]rotaxane; PVL, poly(δ-valerolactone).

precipitation. The most important point to note when synthesizing M2R via the rotaxane-from method is that pseudo[2]rotaxane as the initiator keeps its threaded structure during the initiation, propagation and end-capping processes, even with use of the *sec*-ammonium salt/DB24C8 couple. These authors eventually chose the diphenyl phosphate (DPP)-catalyzed living ring-opening polymerization of a cyclic monomer, such as lactone, as the suitable polymer chain in M2R. Kakuchi and colleagues[54] reported that DPP activates cyclic

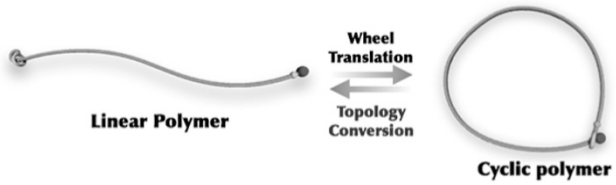

Scheme 4 Synthetic strategy of a cyclic polymer via the topology transformation of macromolecular [1]rotaxane (M1R). A full colour version of this figure is available at the *Polymer Journal* journal online.

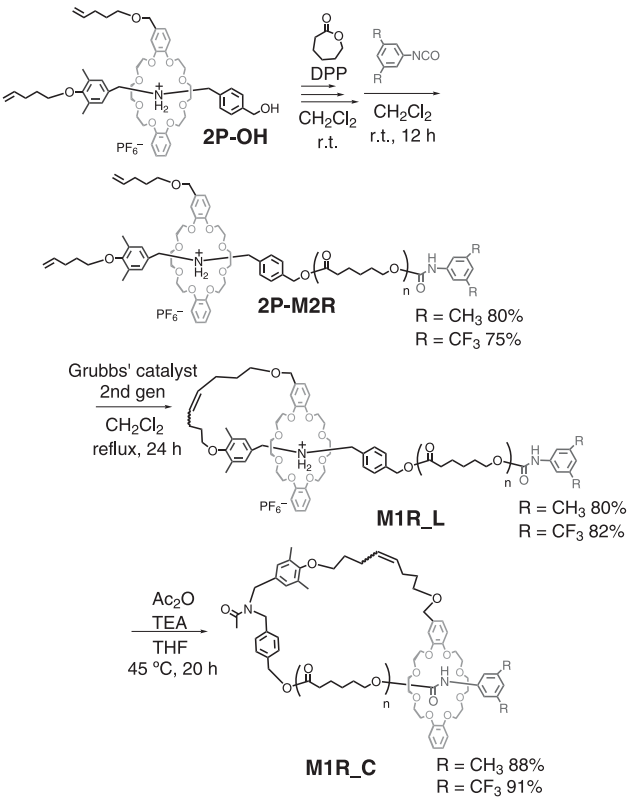

Scheme 5 Synthesis of the cyclic polymer **M1R_C** via the topology transformation of **M1R_L**. M1R, macromolecular [1]rotaxane. A full colour version of this figure is available at the *Polymer Journal* journal online.

monomers, such as δ-valerolactone (VL) and ε-caprolactone (CL), to facilitate the nucleophilic attack of the alcoholic initiator and propagating end to produce the corresponding polymer, that is, poly(δ-valerolactone) (PVL) and poly(ε-caprolactone), respectively, via living polymerization.

To use the pseudo[2]rotaxane containing DB24C8/*sec*-ammonium salt as the initiator for the DPP-catalyzed polymerization, pseudo[2]rotaxane **1-OH**, possessing a *sec*-ammonium salt axle with a primary hydroxyl group, was designed and synthesized, as shown in Scheme 2. As the polymerization proceeded under relatively weaker acidic conditions, **1-OH** efficiently initiated the ring-opening polymerization (ROP) of VL without any decomposition. End-capping of the propagating OH terminal (**PVL-OH**) with bulky isocyanate afforded a *sec*-ammonium salt/crown ether-based M2R with a PVL axle. The purification of M2R by precipitation in a poor solvent was simple but sufficiently effective to remove almost all impurities, such as monomers and bulky isocyanates. A *sec*-ammonium/crown ether-based M2R with a poly(ε-caprolactone) axle was also prepared by the same procedure, but using

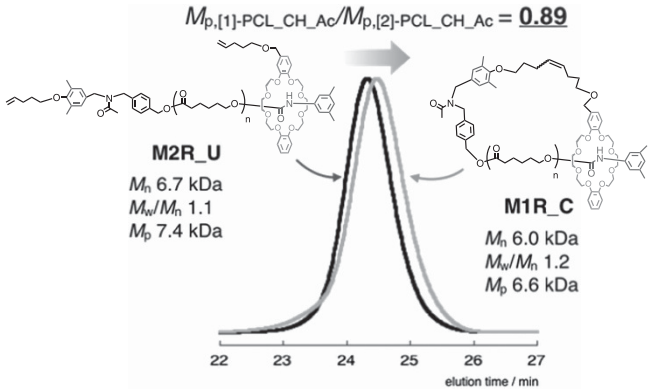

Figure 12 Gel permeation chromatography (GPC) profiles of the linear (**M2R_U**) and cyclic (**M1R_C**) polymers (polystyrene standards; $CHCl_3$ eluent; refractive index (RI) detection). M2R, macromolecular [2]rotaxane. A full colour version of this figure is available at the *Polymer Journal* journal online.

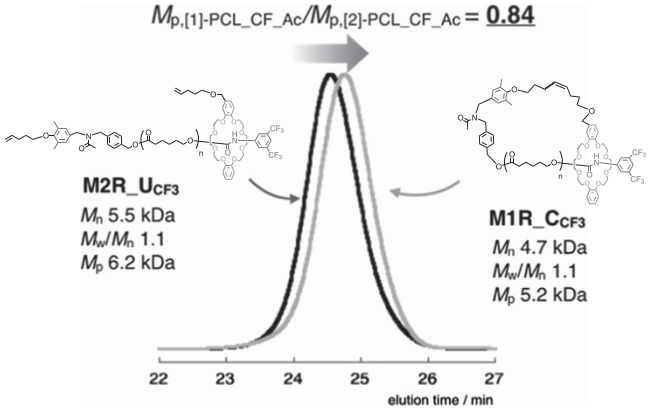

Figure 13 Gel permeation chromatography (GPC) profiles of the linear (**M2R_U$_{CF3}$**) and cyclic polymers (**M1R_C$_{CF3}$**) (polystyrene standards; $CHCl_3$ eluent; refractive index (RI) detection). M2R, macromolecular [2]rotaxane. A full colour version of this figure is available at the *Polymer Journal* journal online.

CL as a monomer instead of VL. Interestingly, the supramolecular initiator **1-OH** did not affect the rate of the DPP-catalyzed polymerization, keeping with the living nature, as demonstrated by the kinetic study. Namely, Takata and colleagues[35] established a novel synthetic method for M2R via a one-pot reaction with a high isolated yield (76–91%).

CHARACTERIZATION OF M2R

The most intriguing property of M2R is the dynamic nature of the components; thus, the mobility of the components of **M2R_F** was enhanced by converting the ionic nitrogen moiety to a nonionic moiety via *N*-acetylation (Scheme 3).

Figure 9 shows the matrix-assisted laser desorption/ionization time-of-flight mass spectrometry spectra of **M2R_F** and **M2R_M**. The series of *m/z* peaks showed a clear molecular weight interval assignable to the PVL unit that possessed both the pseudo[2]rotaxane initiator and the end-cap groups, demonstrating the successful syntheses of perfectly pure **M2R_F** and **M2R_M**.

The component mobility-dependent property of these polymers is interesting. To evaluate the effect of the component mobility in **M2R**, the crystallinity of the axle polymer (PVL) as a suitable probe that is greatly affected by the component mobility was measured by differential scanning calorimetry.[55] Table 1 summarizes the synthesis of **M2R**s with different axle chain lengths, as well as their thermal properties characterized by differential scanning calorimetry (Figure 10). In Table 1, the 10 in **M2R10**, for example, indicates the degree of polymerization (DP = 10) calculated by ^1H nuclear magnetic resonance.

Single endothermic peaks originating from the phase transition of the PVL moiety from crystal to amorphous were observed at 38–60 °C in the differential scanning calorimetry profiles of **M2R_F**s with a DP >15 and **M2R_M**s with a DP >20. This result suggests that PVL moieties with axles shorter than DP 15 cannot form a folded lamellar crystal. Meanwhile, the difference in crystallinity between **M2R20_F** (crystalline) and **M2R20_M** (amorphous) should be attributed to the change in the mobility of the components. Although the melting temperature (T_m) and enthalpy (ΔH_m) values in Table 1 showed little difference between **M2R_F** and **M2R_M** with DPs >35, the rate of crystallization, as characterized by their isothermal crystallization kinetics, was significantly different depending on the mobility difference, as shown in Figure 11.

Figure 11 shows the time-dependent normalized crystallinity of **M2R**s. A movable wheel clearly disturbed the crystallization even when the PVL axle chain with 100 DP was applied. Surprisingly, **M2R_F** (**M2R50_F** and **M2R100_F**) showed similar crystallization behaviors to the model polymers that have the same DP but no wheel component: **PVL-I** with a *sec*-ammonium structure and **PVL-N** with a *N*-acetylated structure (Figure 11a). We thus concluded that the wheel component does not affect the crystallization of PVL in **M2R_F** because the wheel component is fixed at the end of the axle polymer chain via the strong *sec*-ammonium/DB24C8 interaction. In contrast, in **M2R_M**, the presence of the wheel component hindered the crystallization of PVL because the wheel component can move freely along the axle polymer chain in the beginning, but after that, crystallization proceeds over time along the sigmoidal curve after a certain short induction period (Figure 11). In the later part of crystallization, the wheel component is forced to gradually move to the end of the polymer chain as the crystallization progresses, and, eventually, the crystallization completes when the wheel remains at the end of the polymer chain.

Thus, the wheel component disturbs the axle polymer crystallization when the wheel is movable but hardly disturbs the crystallization when the wheel is fixed at the end of the axle terminal.

APPLICATION OF M2R

Unimolecular linking directed toward a linear–cyclic polymer topology transformation

The linear–cyclic polymer topology transformation is discussed as an application of M2R in this section, although it does not directly correspond to the linear–branched topology transformation. This can be regarded as an analogous system to the linear–branched system shown in Figure 6b, in which the axle polymer is directly connected to the wheel component instead of introducing another polymer chain into the wheel component of M2R that is categorized as 'unimolecular linking'. The topology-transformable nature of rotaxane-linked polymers enables the synthesis of cyclic polymers from linear polymers.[56–58] Although cyclic polymers have attracted much interest in both polymer synthesis and physics, the synthesis of cyclic polymers has long suffered from the difficulties of tedious preparation and troublesome purification.[12,59,60] Generally, the synthesis of cyclic polymers is accomplished using two major methods: the cyclization of linear-shaped precursors with a homo or hetero bifunctional group

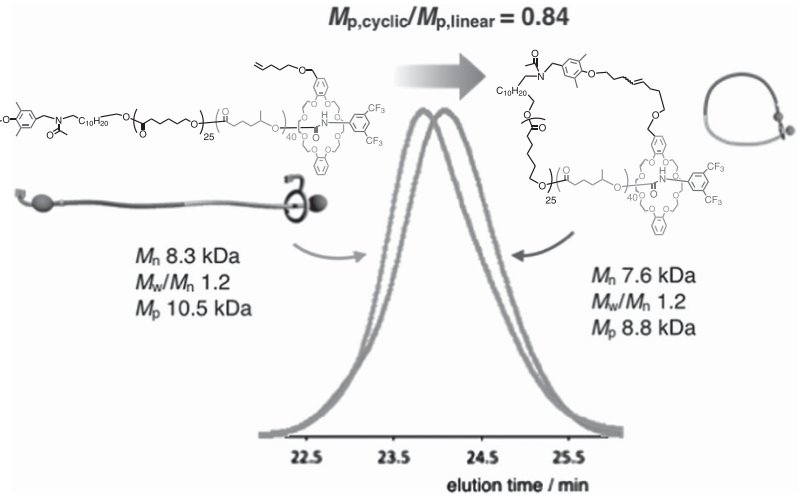

Figure 14 Gel permeation chromatography (GPC) profiles of the linear and cyclic block copolymers (polystyrene standards; $CHCl_3$ eluent; refractive index (RI) detection). A full colour version of this figure is available at the *Polymer Journal* journal online.

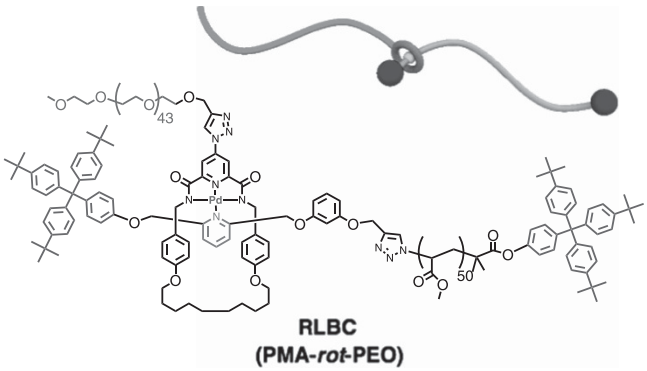

Figure 15 Structure of the rotaxane-linked block copolymer (**RLBC**) synthesized by Fustin and colleagues.[34] A full colour version of this figure is available at the *Polymer Journal* journal online.

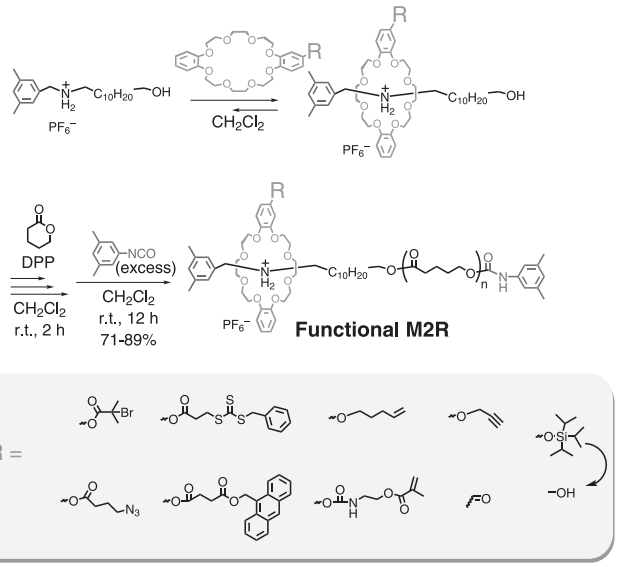

Scheme 6 Synthesis of a macromolecular [2]rotaxane (M2R) containing functional groups. A full colour version of this figure is available at the *Polymer Journal* journal online.

at both ends and ring expansion polymerization through the continuous addition of monomers to the cyclic initiator. Although the cyclization of linear-shaped precursors is the most commonly used method, it requires high reactivity at both polymer ends and efficient cyclization under high dilution conditions to prevent intermolecular reactions. Moreover, the process to isolate the pure cyclic polymer from the mixture containing both the resulting cyclic polymer and unreacted linear precursor is also troublesome. Meanwhile, most ring expansion polymerizations do not provide a well-controlled molecular weight and polydispersity. These defects have prevented the effective synthesis and characterization of cyclic polymers. Recently, we developed a novel strategy for effective cyclic polymer synthesis based on the structural transformation of macromolecular [1]rotaxane (M1R) that is obtained by linking a wheel component and an axle component of M2R (Scheme 4).

As this cyclization strategy involves the transportation of the wheel component along the polymer axle of M1R, the efficiency is 100% irrespective of concentration that differs from the cyclization between the two polymer ends. The initial small cyclic part of the linear M1R (**M1R_L**) is gradually expanded according to the translation of the wheel to form a large cyclic polymer. Scheme 5 shows the actual synthetic scheme of the linear polymer **M1R_L** and its topology transformation to the cyclic polymer **M1R_C**.[56]

The pseudo[2]rotaxane initiator (**2P-OH**) composed of *sec*-ammonium with both pentenyl substituents and terminal benzyl alcohol and DB24C8 with pentenyl substituents is a key initiator to synthesize M1R by linking the axle and wheel components. After the DPP-catalyzed living ring-opening polymerization of CL and the end-capping reaction (**2P-M2R**), the ring-closing metathesis of the terminal rotaxane moiety of the obtained M2R yielded the corresponding linear M1R (**M1R_L**). A topology transformation from linear to cyclic was conducted via acetylation of the *sec*-ammonium moiety. The transformation of the wheel component α-end to the ω-end resulted in the successful synthesis of the cyclic polymer (**M1R_C**). The topology transformation was confirmed by GPC, as shown in Figure 12.

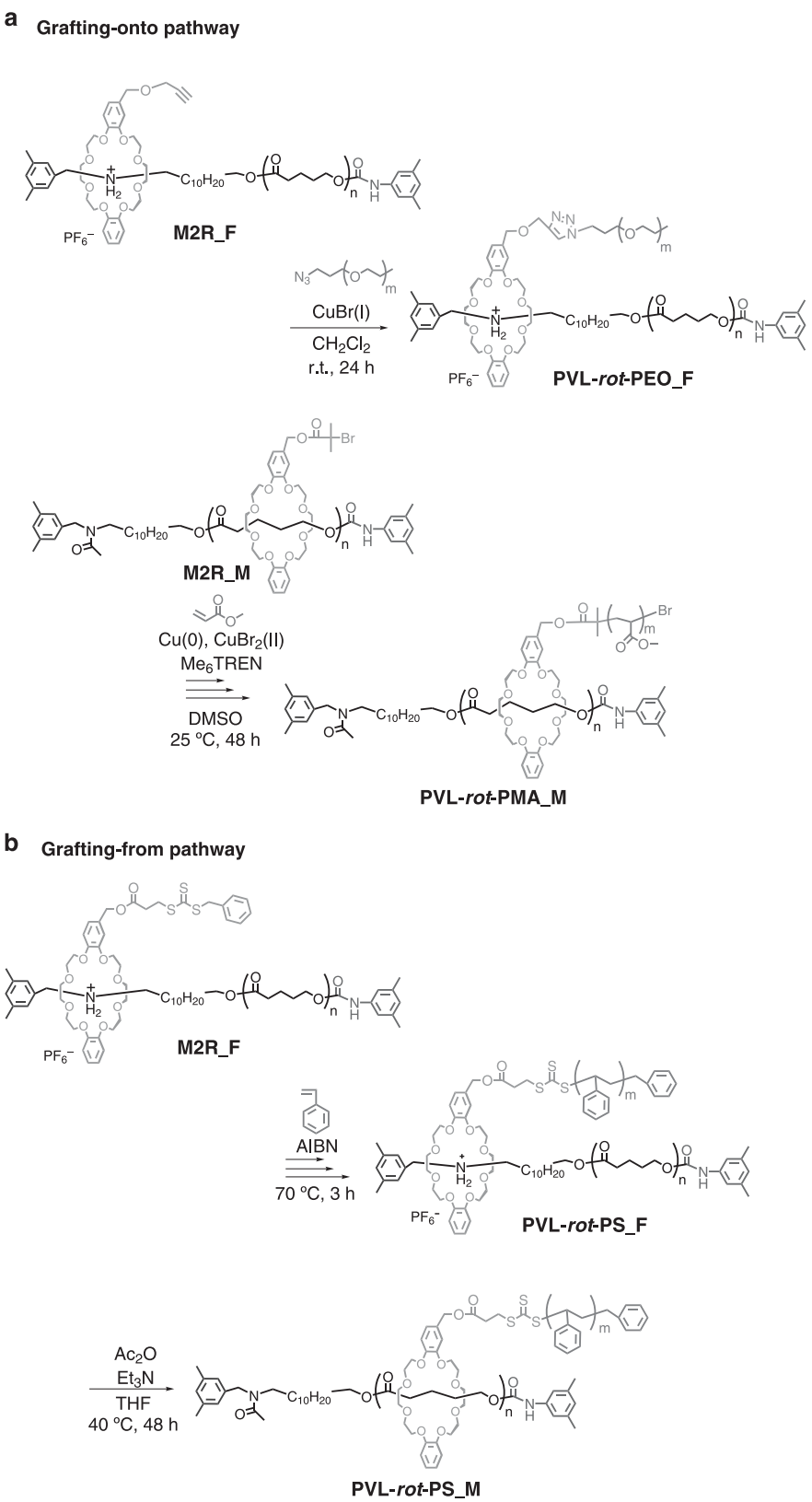

Scheme 7 Syntheses of rotaxane-linked block copolymer (RLBC) via the (**a**) grafting-onto and (**b**) grafting-from pathways. A full colour version of this figure is available at the *Polymer Journal* journal online.

The GPC profile of **M1R_C** showed a smaller molecular weight distribution than that of the linear model (**M2R_U**), clearly supporting the polymer topology change from linear to cyclic. The cyclic structure was also supported by the change in the degree of cyclization, whereby **M1R_C$_{CF3}$**, which possesses enhanced acidity because of the addition of a terminal urethane moiety by the substitution of the dimethylphenylurethane moiety with the electron-withdrawing bis(trifluoromethyl)phenylurethane moiety, obviously had a higher level cyclic structure than **M1R_C** (Figures 12 and 13).

The linear–cyclic polymer topology transformation was also applied to the synthesis of a cyclic block copolymer using CL and hexanolactone as the monomers.[58] The similar GPC profile change (Figure 14) suggested the development of an effective synthetic method of cyclic polymers containing two polymer components. The change in the crystallinity of the polymer upon cyclization also confirmed the efficient topological change, and the cyclic polymer had a higher melting point than linear one.

Bimolecular linking directed toward the linear–branched polymer topology transformation

M2R can be applied to the synthesis of RLBCs. Fustin and colleagues[34] reported the synthesis of a RLBC (PMA-*rot*-PEO) composed of poly (methyl acrylate) (PMA) and poly(ethylene oxide) (PEO), in which both are connected with a rotaxane structure (Figure 15). They used '*-rot-*' to distinguish RLBC from other block copolymers connected with covalent bonds and supramolecular interactions, such as hydrogen bonding and coordination bonding. We applied the rotaxane-from method to the synthesis of a variety of RLBCs by introducing various polymer chains into the components of M2R.[61]

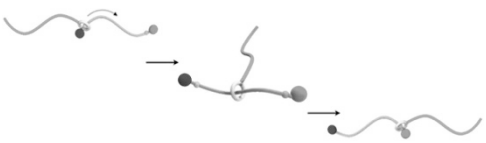

Figure 16 Structural transformation of rotaxane-linked block copolymer (RLBC) via the relative positional change of the wheel component from the α-end to the ω-end. A full colour version of this figure is available at the *Polymer Journal* journal online.

To introduce an additional polymer chain onto the wheel component of M2R, various functional groups were introduced into the crown ether wheel that was complexed with a *sec*-ammonium salt containing a hydroxyl group to produce a pseudorotaxane initiator for the living ring-opening polymerization of VL, as shown in Scheme 6. The polymerization and successive end-capping resulted in the formation of functionalized M2Rs with relatively high isolated yields and high purity. Scheme 7 shows the synthetic methods of RLBCs via two methods, that is, grafting-from and grafting-onto, to yield the RLBCs **PVL-*rot*-PEO_F** and **PVL-*rot*-PS_F** (polystyrene (PS)). Furthermore, the *sec*-ammonium moiety of the RLBCs was acetylated to allow the wheel component containing the polymer chain to move along the axle polymer chain (**PVL-*rot*-PS_M**) (Scheme 7b).

We first studied the dynamic nature of RLBC. The effect of the change in the polymer structure on the solution properties of RLBC by *N*-acetylation-induced neutralization or mobility enhancement was evaluated by GPC. No large effect was observed as the GPC result did not show a peak shift, in good agreement with the nearly equal polymer chain length of RLBCs before and after *N*-acetylation (Figure 16). The attractive interaction of the wheel component containing the urethane group located at the ω-end of the axle polymer chain produces the same copolymer chain length as that located at the α-end before *N*-acetylation. If there is no point on the axle polymer that is attractive for the wheel component, the average topology of RLBC would be branched at the rotaxane junction, rather than linear, and RLBC is expected to show a smaller hydrodynamic volume than the linear one (Figure 16). This topic will be discussed again in a later section.

To obtain more information, a rotaxane-linked polymer containing the same polymer chains in both the axle and wheel components was prepared.[62] Two hydroxyl group-tethered pseudorotaxane initiators (**2-OH**) underwent the DPP-catalyzed living ring-opening polymerization of VL, and the successive end-capping reaction with 3,5-dimethylphenyl isocyanate afforded rotaxane-linked homopoly(valerolactone), **2-PVL_F** (Scheme 8).

The spectral characterization of **2-PVL_F** agreed with the proposed structure, in which the two PVL chains on the components had the same degree of polymerization. Surprisingly, a rotaxane-linked PVL

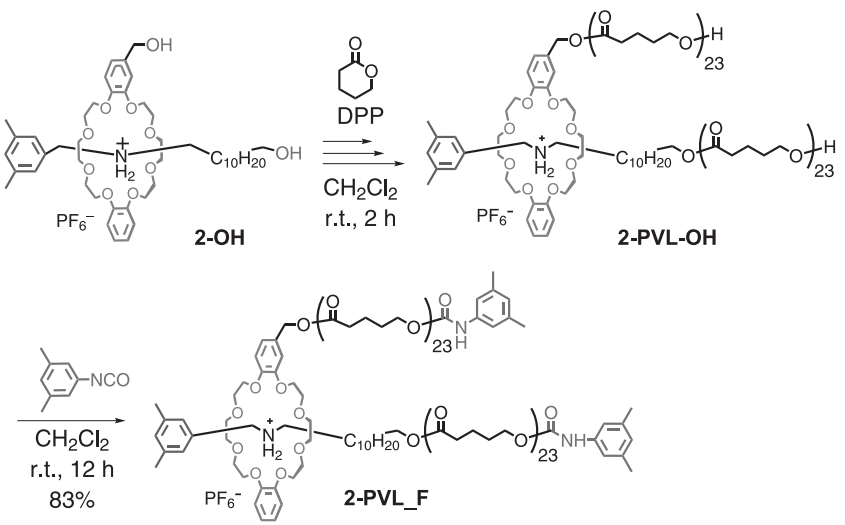

Scheme 8 Synthesis of rotaxane-linked PVL **2-PVL_F** by the rotaxane-from method. PVL, poly(δ-valerolactone). A full colour version of this figure is available at the *Polymer Journal* journal online.

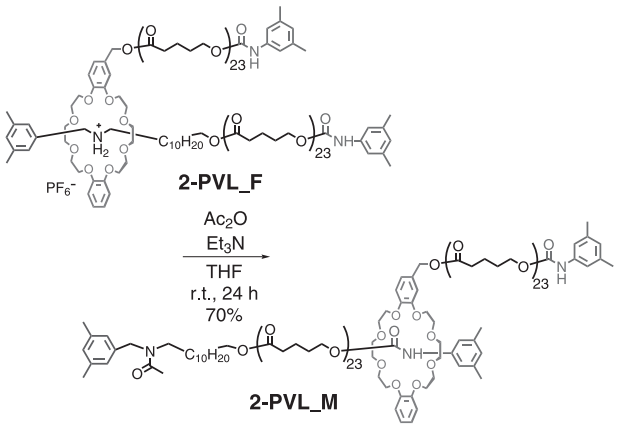

Scheme 9 Synthesis of **2-PVL_M**. PVL, poly(δ-valerolactone). A full colour version of this figure is available at the *Polymer Journal* journal online.

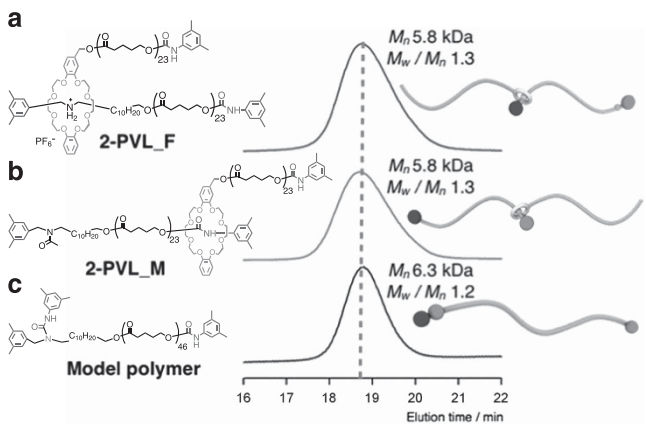

Figure 17 Gel permeation chromatography (GPC) profile of (**a**) **2-PVL_F**, (**b**) **2-PVL_M** and (**c**) the model polymer ($CHCl_3$, PSts). PVL, poly(δ-valerolactone). A full colour version of this figure is available at the *Polymer Journal* journal online.

without bulky end-cap groups (**2-PVL-OH**) was also isolated by precipitation. No deslippage of the wheel component from the axle component was confirmed during the isolation process, and **2-PVL-OH** was stably isolated, clearly demonstrating the excellent strength of the *sec*-ammonium/DB24C8 interaction. Then, **2-PVL_F** was neutralized by *N*-acetylation to afford **2-PVL_M**, in which the wheel component was mobile along the axle chain (Scheme 9).

The dynamic nature of **2-PVL_F** and **2-PVL_M** was evaluated by GPC (eluent: $CHCl_3$) for comparison with the corresponding model linear polymer having a DP of VL equal to the sum of the DP of the two polymer units of **2-PVL**. **2-PVL_F** and **2-PVL_M** showed very similar GPC profiles and molecular weights (Figure 17), which is in good agreement with the results discussed above and as seen in the case of RLBC, indicating that these polymers have a similar hydrodynamic volume. Considering the strong intercomponent interaction, **2-PVL_F** will act as a linear-shaped polymer in a less polar solvent, such as $CHCl_3$.

This assumption was evidently proven by a similar GPC result of the model polymer, suggesting that **2-PVL_M** also has a linear topology. As mentioned above, the urethane group at the ω-end of the axle polymer in **2-PVL_M** fixes the wheel component at the ω-end, making the

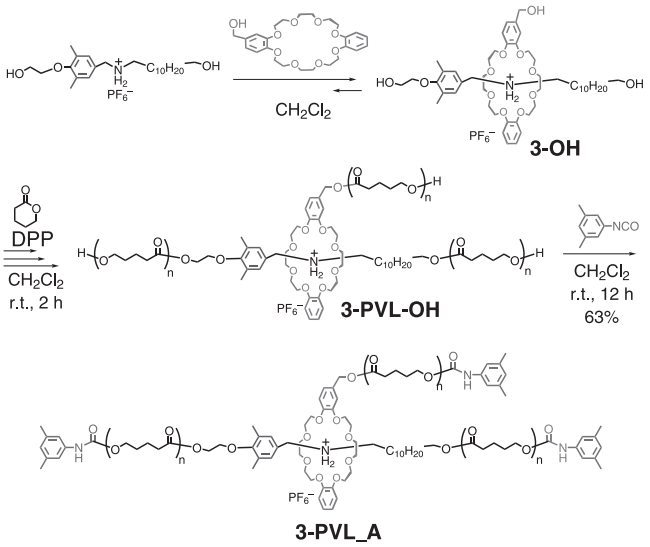

Scheme 10 Synthesis of rotaxane-linked star polymer (**3-PVL_A**). PVL, poly (δ-valerolactone). A full colour version of this figure is available at the *Polymer Journal* journal online.

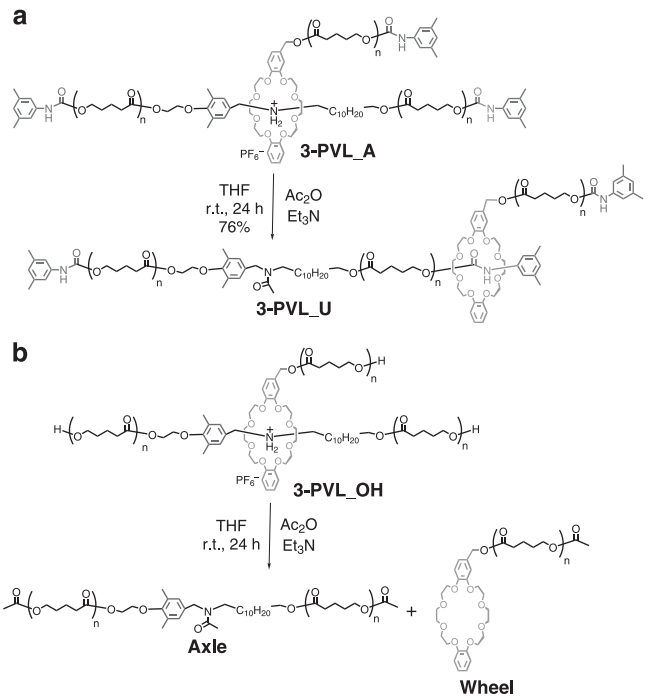

Scheme 11 Topology transformation of star-shaped **3-PVL_A** to linear **3-PVL_U** by *N*-acetylation. PVL, poly(δ-valerolactone). A full colour version of this figure is available at the *Polymer Journal* journal online.

entire polymer topology linear, similar to that before *N*-acetylation. In the urethane group/crown ether interaction, Gibson and colleagues[63–66] reported that the formation of hydrogen bonds between the urethane NH group and the crown ether wheel resulted in the generation of a significant thermodynamic driving force for the threading complexation. These reports support the present transfer of the wheel component-tethered polymer chain from the α-end to the ω-end of the axle polymer by removing the *sec*-ammonium/DB24C8 interaction.

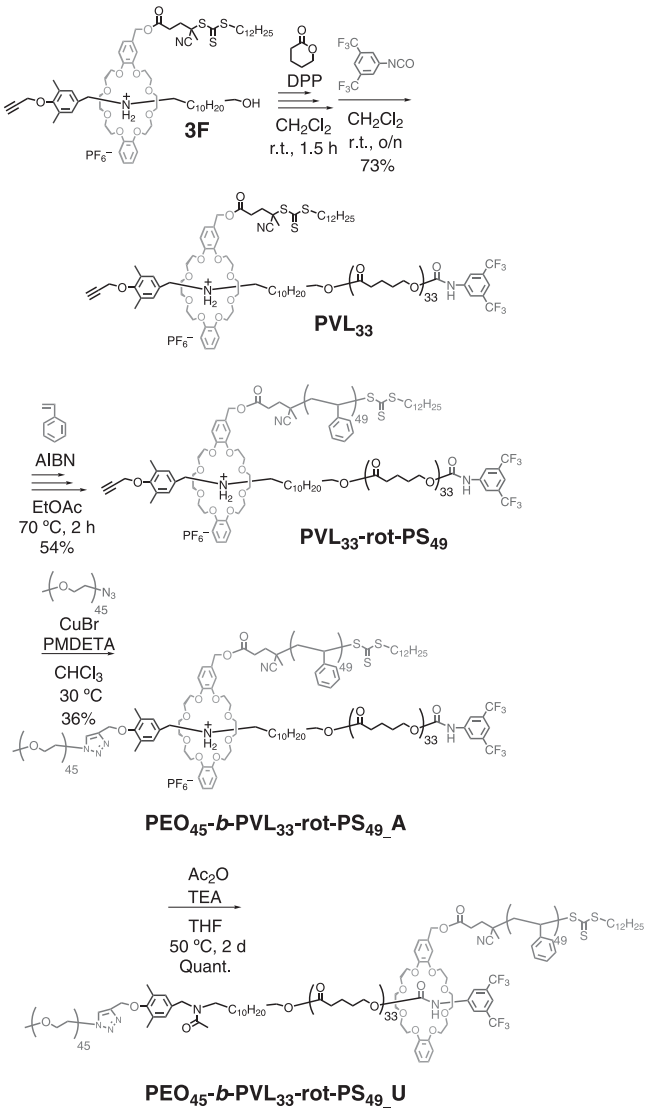

Scheme 12 Synthesis of rotaxane-linked ABC star terpolymers. A full colour version of this figure is available at the *Polymer Journal* journal online.

Trimolecular linking directed toward the linear–branched (Star) polymer topology transformation

Polymer topology transformations, which change the essential molecular shape of a polymer, for example, from a cyclic to a linear structure (section 'Unimolecular linking directed toward a linear–cyclic polymer topology transformation'), often cause large macroscopic property changes, both in bulk and in solution. Although topology-changeable molecules have been limited mainly to small molecules until 2000, recent progress in synthetic organic and polymer chemistry has made the topology change of polymer molecules possible,[67–70] as discussed in the section 'Bimolecular linking directed toward the linear–branched polymer topology transformation'. Compared with linear polymers, corresponding polymers with different topologies, such as star polymers,[71–73] cyclic polymers,[12,59,60] dendrimers[74–76] and hyperbranched polymers,[16] generally have a smaller hydrodynamic volume, lower solution viscosity and less polymer entanglement in bulk. Therefore, the development of topology-transformable polymers in response to a specific stimulus is particularly attractive to control the polymer properties and to construct novel stimuli-responsive materials.[77–80]

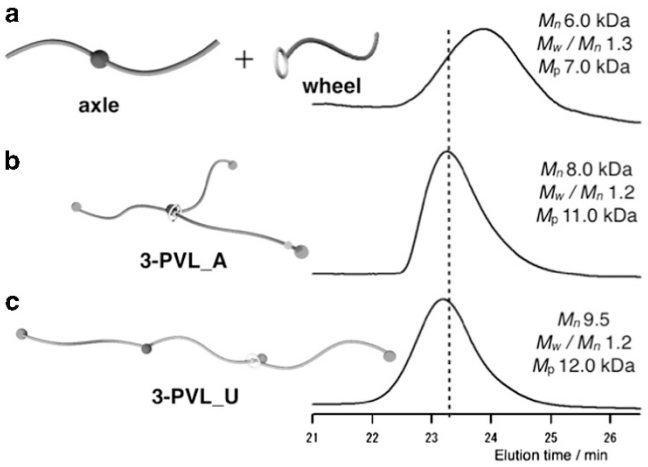

Figure 18 Gel permeation chromatography (GPC) profiles of (**a**) *N*-acetylated **3-PVL-OH**, (**b**) **3-PVL_A** and (**c**) **3-PVL_U** calibrated with polystyrene standards ($CHCl_3$ eluent; refractive index (RI) detection). PVL, poly(δ-valerolactone). A full colour version of this figure is available at the *Polymer Journal* journal online.

We first describe our results for the topology-transformable 3-arm star polymer derived from a crown ether-based M2R with *sec*-ammonium and urethane moieties on the polymer axle that can be regarded as a two-station-type molecular switch.[81] As shown in Scheme 10, the topology-transformable star polymer (**3-PVL_A**) was synthesized using the trifunctional pseudo[2]rotaxane initiator **3-OH**, which contains three primary OH groups, to ensure the synthesis of the well-defined three-armed star polymer **3-PVL-OH** in which the arm polymer chains have the same DP. Treatment of the three terminal OH groups of the polymer with a bulky isocyanate gave the corresponding star polymer **3-PVL_A**, in which the polymer chain on the wheel component is fixed at the center of the axle polymer chain by the *sec*-ammonium/crown ether interaction.

The topology transformation of the star polymer **3-PVL_A** to the linear polymer **3-PVL_U** was achieved by changing the intercomponent interaction from *sec*-ammonium moiety/crown ether to urethane moiety/crown ether via the simple *N*-acetylation of **3-PVL_A** (Scheme 11a). Meanwhile, the similar treatment of a rotaxane-linked star polymer that did not contain bulky end-cap groups (**3-PVL-OH**) resulted in the decomposition of the rotaxane structure by acetylation of the corresponding wheel and axle components (Scheme 11b). Figure 18 shows the GPC profiles of the product mixtures obtained from the *N*-acetylation of **3-PVL-OH**, **3-PVL_A** and **3-PVL_U**. The broad GPC peak of acetylated **3-PVL-OH** eluted at a lower molecular weight region compared with those of **3-PVL_A** and **3-PVL_U**, suggesting the decomposition of **3-PVL-OH** to the two polymers connected to the axle and wheel components because of the absence of the bulky end-cap. This result in turn evidently reveals that the wheel component carrying a polymer chain readily moves along the axle polymer chain to the polymer end and is eventually threaded out from the polymer end by being released from the strong intercomponent interaction of *sec*-ammonium/crown ether.

Meanwhile, the unimodal peak of **3-PVL_U** appeared at an earlier elution time than that of **3-PVL_A** without a change in M_w/M_n. We concluded that this peak shift is caused by an increase in the hydrodynamic volume, clearly supporting the occurrence of the topology transformation from star shaped to linear. The topology

transformation was also supported by the viscosity change. Covalently connected star and linear model polymers were also prepared for comparison, as shown in Figure 19. The increased intrinsic viscosity [η] of **3-PVL_U** over that of **3-PVL_A** indicated the topology transformation from a star polymer to a linear polymer, and the g' value (ratio of the intrinsic viscosity of the covalently connected star and linear polymers with same molecular weights) was similar to that of the model polymers. The report presented the first topology-transformable polymer, again emphasizing the importance of the basic rotaxane polymer M2R.

Compared with the rotaxane-linked polymers tethered with the same polymer chain structures described above, rotaxane-linked polymers containing different polymer chain structures, such as block star polymers, have attracted great interest from both a scientific and practical perspective. In particular, star polymers composed of three different types of polymer chains show unique characteristics, such as microphase-separated structures, owing to their topology that cannot be attained by their linear analogs, as reported by Matsushita and

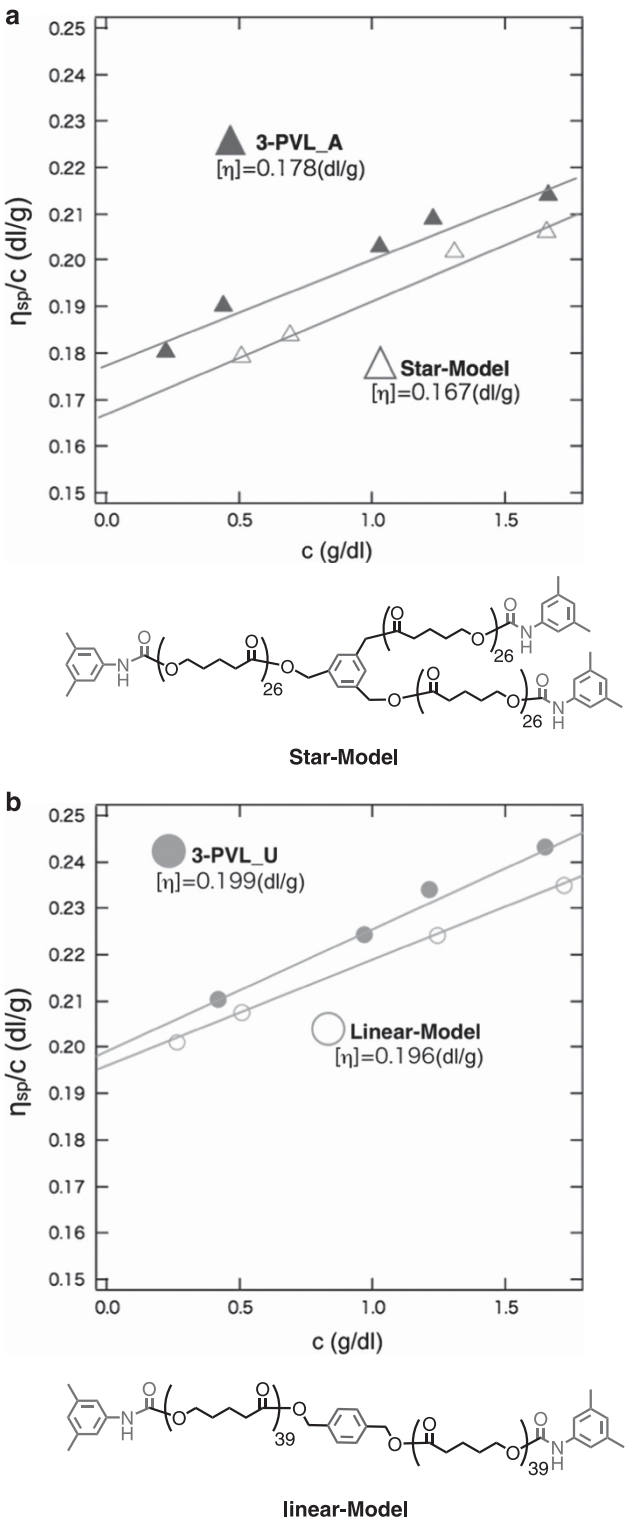

Figure 19 Huggins plots of (**a**) **3-PVL_A** and the star model and (**b**) **3-PVL_U** and the linear model (measured in $CHCl_3$). PVL, poly(δ-valerolactone). A full colour version of this figure is available at the *Polymer Journal* journal online.

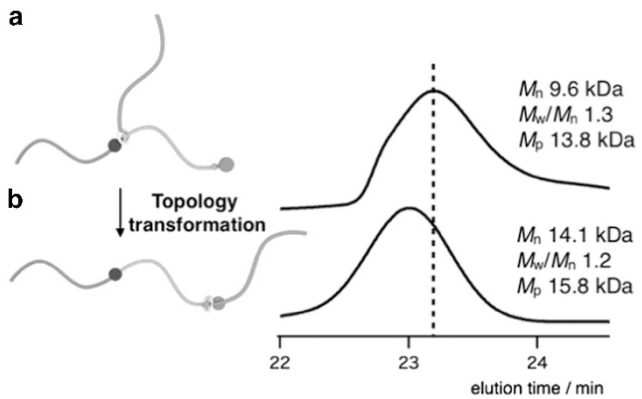

Figure 20 Gel permeation chromatography (GPC) profiles of the (**a**) rotaxane-linked star terpolymer (**PEO_{45}-*b*-PVL_{33}-rot-PS_{49}_A**) and (**b**) rotaxane-linked linear terpolymer (**PEO_{45}-*b*-PVL_{33}-*rot*-PS_{49}_U**) calibrated using polystyrene standards ($CHCl_3$ eluent; refractive index (RI) detection). A full colour version of this figure is available at the *Polymer Journal* journal online.

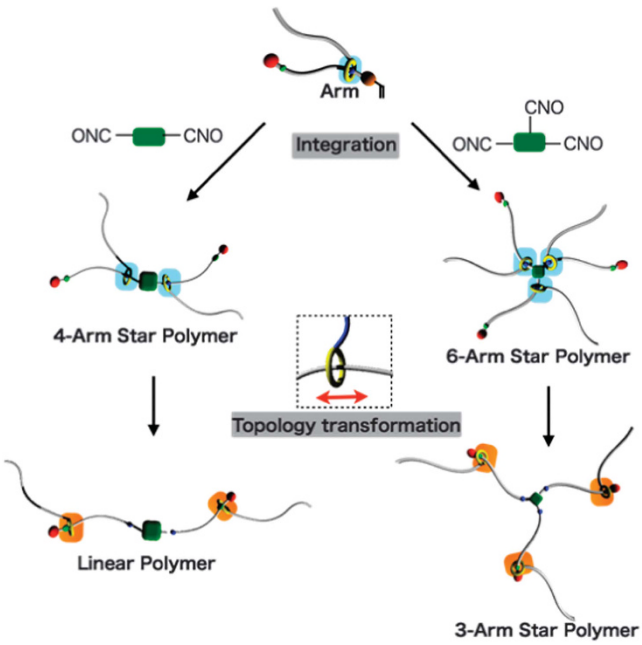

Figure 21 Synthesis and structural transformation of 4- and 6-arm star polymer systems based on rotaxane-linked arm polymer chains.

colleagues.[32,33] To extend the capability and applicability of the topology-transformable systems based on M2R, we synthesized a topology transformable ABC terpolymer.[82] A pseudo[2]rotaxane initiator (**3F**) capable of linking three polymer chains by the rotaxane linkage was designed as the key trifunctional compound for the star polymer synthesis (Scheme 12).

The living ring-opening polymerization of VL initiated with **3F** and successive capping of the propagating end was followed by the

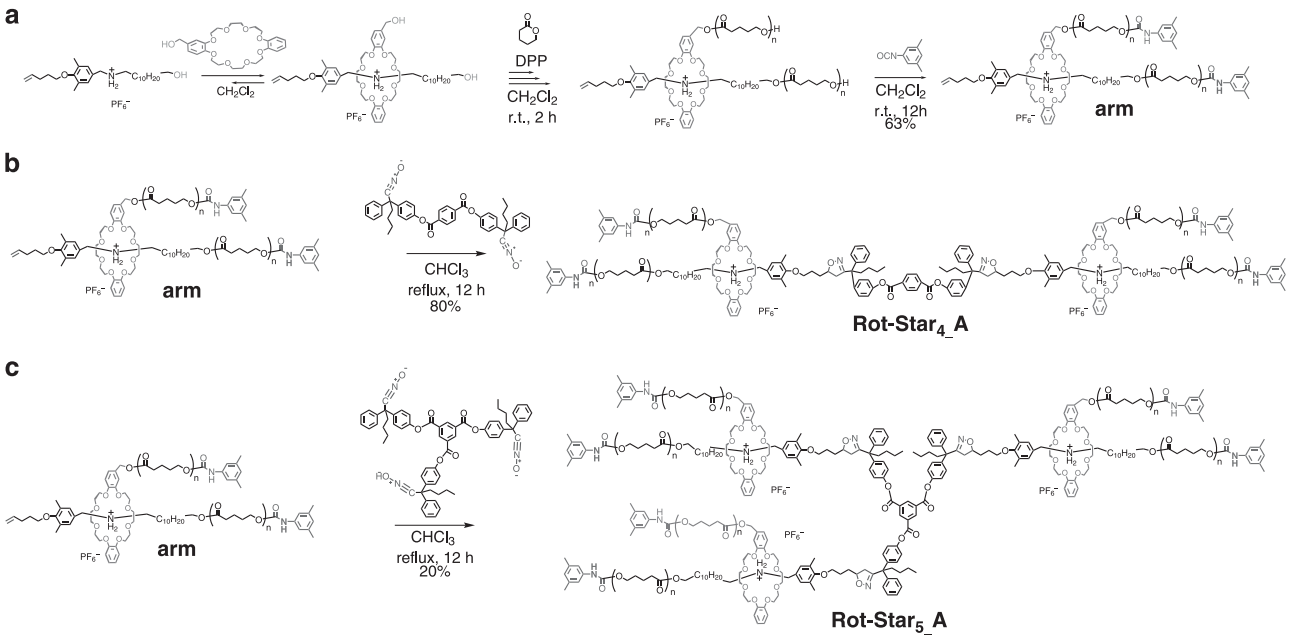

Scheme 13 Syntheses of a (**a**) structure-transformable unit (**arm**), (**b**) 4-arm rotaxane-linked star polymer (**Rot-Star$_4$_A**) and (**c**) 6-arm rotaxane-linked star polymer (**Rot-Star$_6$_A**). A full colour version of this figure is available at the *Polymer Journal* journal online.

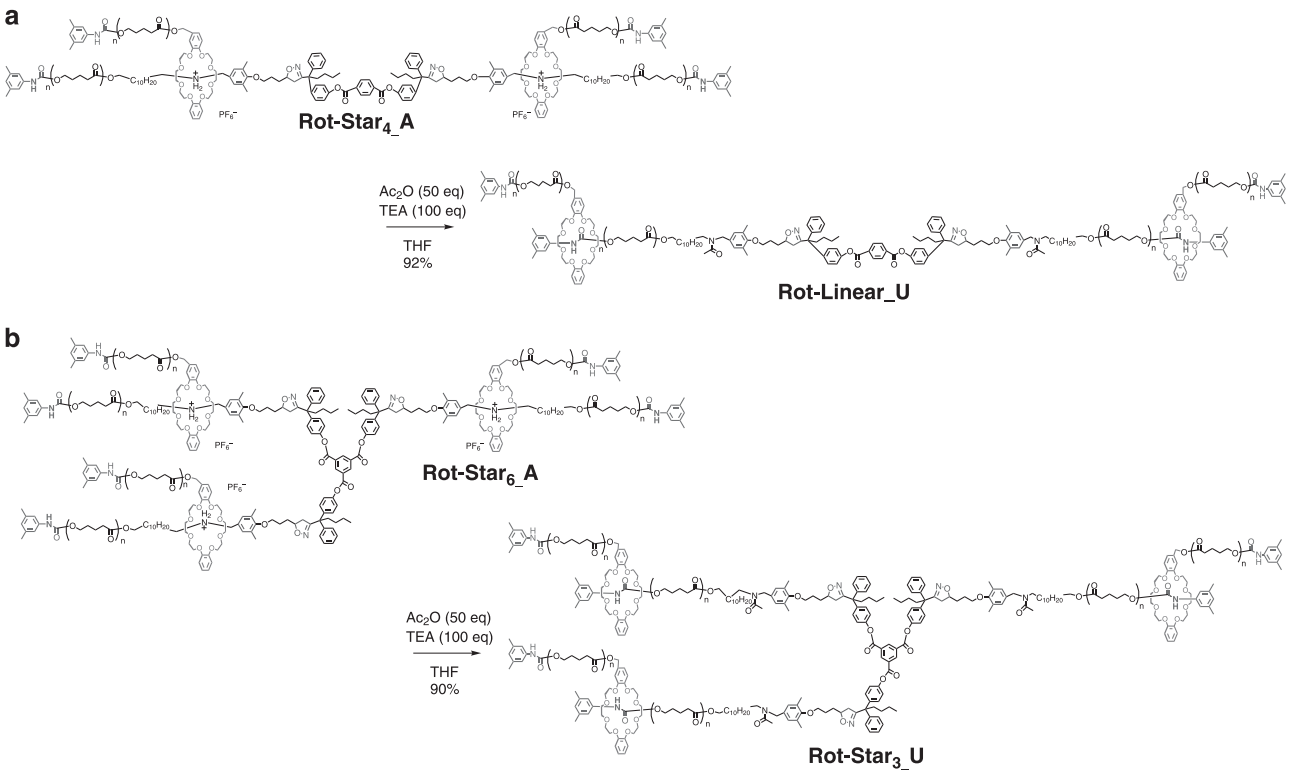

Scheme 14 Structural transformation (**a**) from a 4-arm star to linear and (**b**) from a 6-arm star to a 3-arm star polymer. A full colour version of this figure is available at the *Polymer Journal* journal online.

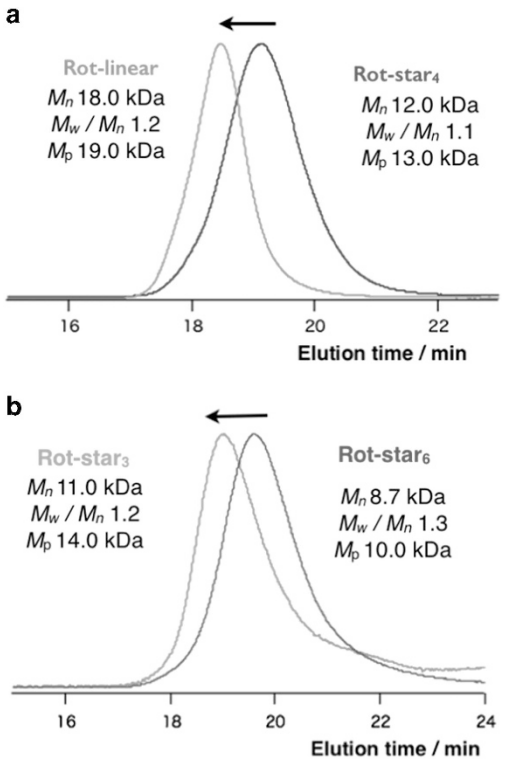

Figure 22 Gel permeation chromatography (GPC) profiles before and after the acetylation of (**a**) **Rot-Star$_4$_A** and (**b**) **Rot-Star$_6$_A** calibrated with polystyrene standards (*N*,*N*-dimethylformamide (DMF) eluent; 0.70 ml min^{-1} flow rate; refractive index (RI) detection). A full colour version of this figure is available at the *Polymer Journal* journal online.

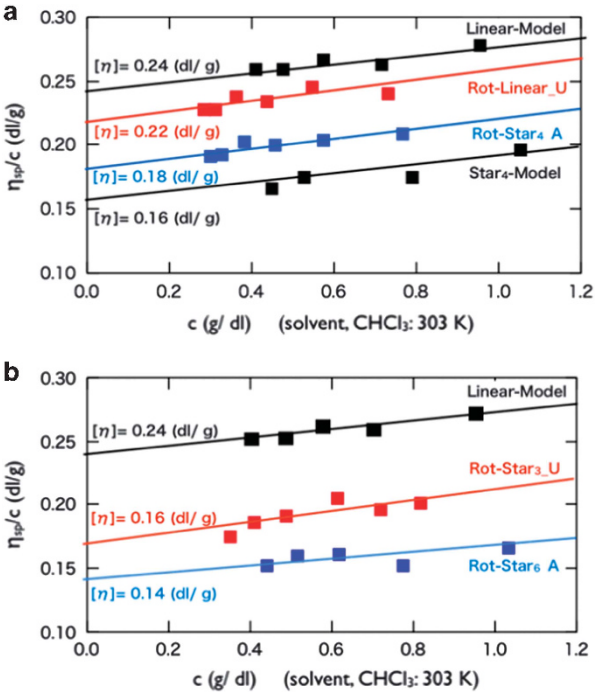

Figure 23 Huggins plots of the star and linear polymers. (**a**) **Rot-Star$_4$_A**, **Rot-Linear_U**, and model polymers **Star$_4$-Model** and **Linear-Model** and (**b**) **Rot-Star$_6$_A** and **Rot-Star$_3$_U**, and model polymer **Linear-Model**.

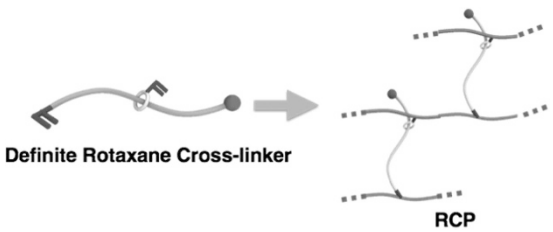

Figure 24 Macromolecular [2]rotaxane (M2R)-based rotaxane crosslinker with a definite structure for the fabrication of a rotaxane crosslinked polymer (RCP). A full colour version of this figure is available at the *Polymer Journal* journal online.

reversible addition–fragmentation chain transfer polymerization of styrene to give the corresponding two polymer chain-tethering [2] rotaxane **PVL$_{33}$-*rot*-PS$_{49}$**.

The final polymer connection via the click reaction with azide-terminated poly(ethylene oxide) afforded the rotaxane-linked ABC star terpolymer **PEO$_{45}$-*b*-PVL$_{33}$-*rot*-PS$_{49}$_A**.

The strong interaction of *sec*-ammonium/DB24C8 fixed the rotaxane-linked structure at the center of the axle polymer chain to connect the arm polymer chains. However, *N*-acetylation of the *sec*-ammonium moiety of **PEO$_{45}$-*b*-PVL$_{33}$-*rot*-PS$_{49}$_A** resulted in the transformation of the initial polymer topology from star shaped to linear (**PEO$_{45}$-*b*-PVL$_{33}$-*rot*-PS$_{49}$_U**) via the emergence of the urethane/crown ether interaction at the end of the axle polymer PVL chain. The peak shift in the GPC profile to the higher molecular weight region strongly supports the structure and dynamic nature of the topology-transformable ABC terpolymer (Figure 20).

Star polymers capable of changing arm number and arm length

As mentioned above, the polymer topology can be changed from a 3-arm star to linear. To extend the capability and applicability of this system, a rotaxane linkage was introduced into the arm polymer chains of multi-arm star polymers as the movable junction point, as the arm number and length are critical factors determining the polymer properties and functionalities. In this section, the synthesis, structural transformation and properties of novel star polymers with changeable arm number and length via the integration of structure-transformable units to the central core are discussed. The integration of structure-transformable units via the highly effective click reaction of nitrile *N*-oxide is an effective way to synthesize multi-arm star polymers (Figure 21).[83–88]

The transformable unit (**arm**) consisting of rotaxane-linked PVL and an alkene group as a reactive group was synthesized via the DPP-catalyzed living ring-opening polymerization of δ-VL initiated by the two hydroxyl groups of a *sec*-ammonium/crown ether-type pseudo[2] rotaxane with an alkene group on the axle component, as shown in Scheme 13a. The two propagating end groups (−OH) were reacted with 3,5-dimethylphenyl isocyanate that not only acts as the bulky end-cap but also produces the second attractive site for the crown ether wheel as the urethane group at the polymer end.

Click reactions of the **arm** obtained with bi- or tri-functionalized nitrile *N*-oxides were conducted to prepare star polymers, as shown in Scheme 13b and c. Simply mixing the nitrile *N*-oxides and alkene-containing **arm**s in chloroform gave the corresponding star polymers, **Rot-Star$_4$_A** (b, > 80%) and **Rot-Star$_6$_A** (c, 20%), after heating for 12 h under reflux.

The structural transformation of the resulting star polymers was achieved by changing the *sec*-ammonium/crown ether interaction to

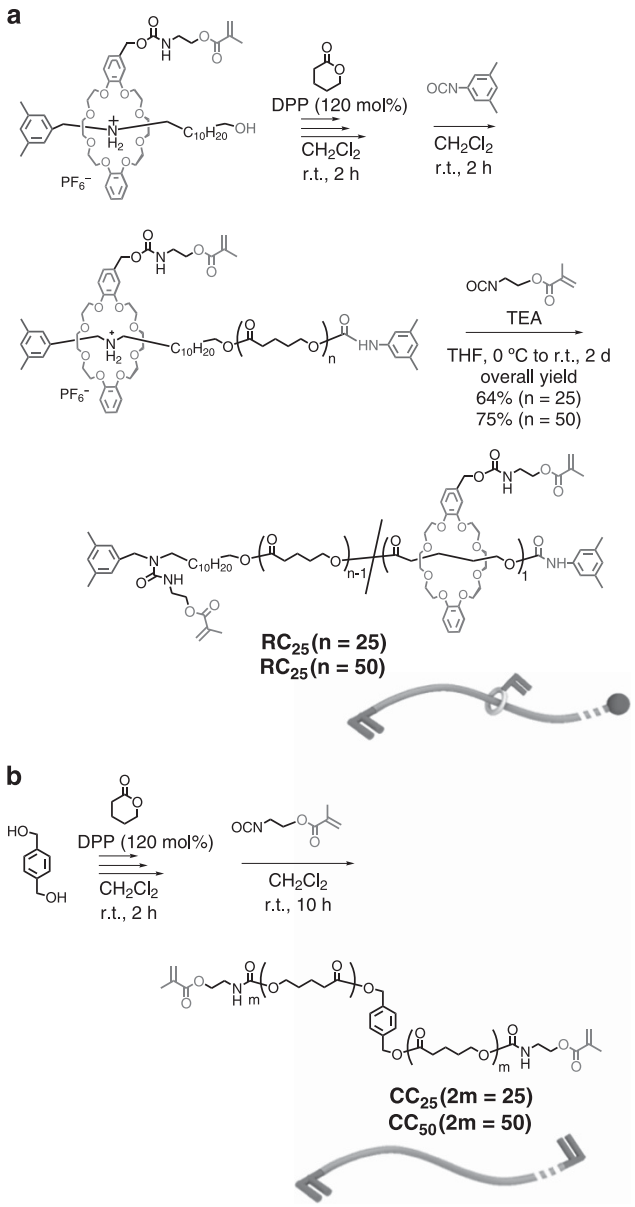

Scheme 15 (**a**) Synthesis of a macromolecular [2]rotaxane (M2R)-based rotaxane crosslinker (RC) and (**b**) the design of a covalent crosslinker (CC) for comparison. A full colour version of this figure is available at the *Polymer Journal* journal online.

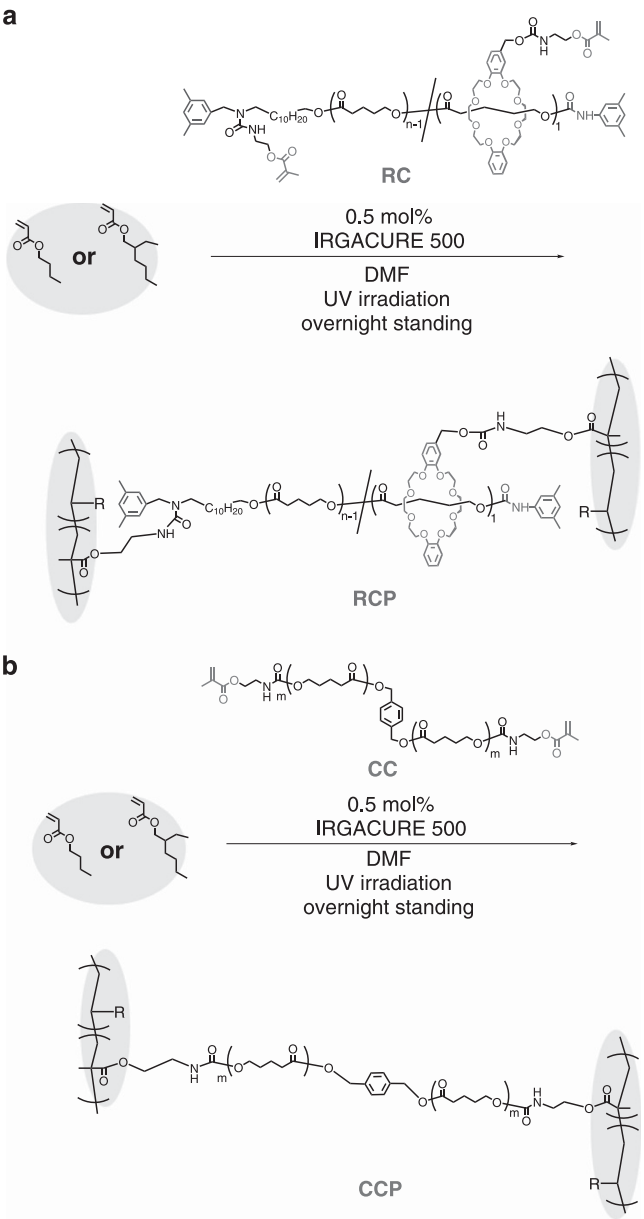

Scheme 16 Synthesis of (**a**) rotaxane crosslinked polymer (RCP) and (**b**) covalently crosslinked polymer (CCP). A full colour version of this figure is available at the *Polymer Journal* journal online.

Table 2 Syntheses of the crosslinkers RC and CC

Crosslinker	*Yield [%]*	$M_{n\ GPC}$ [a] *[kDa]*	M_w / M_n [a]	DP_n [b]	$M_{n\ NMR}$ [b] *[kDa]*
RC$_{25}$ ($n=25$)	64	6.0	1.19	23	3.5
RC$_{50}$ ($n=50$)	75	8.3	1.13	50	6.2
RC$_{25}$ (2m = 25)	88	5.2	1.25	20	2.4
RC$_{50}$ (2m = 50)	98	9.5	1.20	52	5.6

Abbreviations: CC, covalent crosslinker; DP, degree of polymerization; RC, rotaxane crosslinker.
[a]Determined by gel permeation chromatography (GPC) ($CHCl_3$, polystyrene standards).
[b]Determined by ^{1}H nuclear magnetic resonance (NMR).

the urethane/crown ether interaction via *N*-acetylation of the *sec*-ammonium moiety on the axle component (Scheme 14).

In addition to the ^{1}H nuclear magnetic resonance and matrix-assisted laser desorption/ionization time-of-flight mass spectrometry spectra, the GPC profiles before and after *N*-acetylation clearly confirmed the structural transformation (Figure 22): (1) **Rot-Star$_4$_A** to **Rot-Linear_U** and (2) **Rot-Star$_6$_A** to **Rot-Star$_3$_U**. After *N*-acetylation, the GPC peaks of both **Rot-Star$_4$_A** (M_p 12.0 kDa) and **Rot-Star$_6$_A** (M_p 8.7 kDa) shifted to the high molecular weight region (**Rot-Linear_U**, M_p 18.0 kDa; **Rot-Star$_3$_U**, M_p 11.0 kDa) without a change in the M_w/M_n, demonstrating the structural transformation from the 4-arm star polymer to the linear polymer and from the 6-arm star polymer to the 3-arm star polymer with a longer arm length.

Figure 23a shows the Huggins plots of **Rot-Star$_4$_A** and **Rot-Linear_U** along with the model polymers containing covalently connected polymer chains with almost the same molecular weights

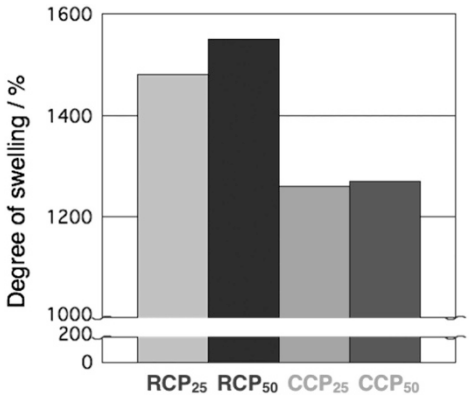

Figure 25 Degree of swelling of poly(*n*-butyl acrylate) (poly(BA))-based rotaxane crosslinked polymers (RCPs) and covalently crosslinked polymers (CCPs) toward $CHCl_3$. A full colour version of this figure is available at the *Polymer Journal* journal online.

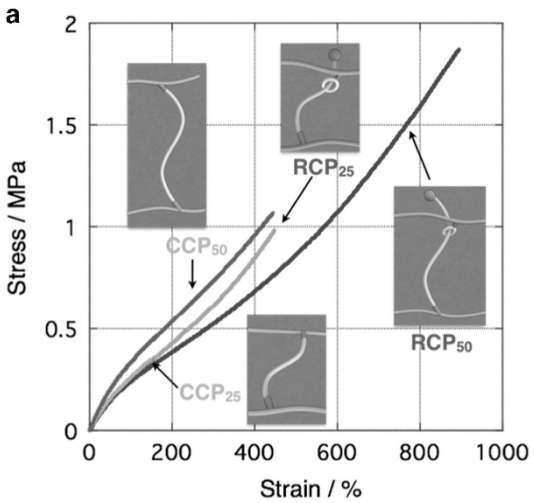

b

Sample	Fracture Strain	Fracture Stress	Fracture Energy	Young's Modulus
RCP_{25}	450	0.98	2.2	0.37
RCP_{50}	890	1.9	7.5	0.34
CCP_{25}	150	0.35	0.3	0.37
CCP_{50}	440	1.1	2.6	0.49

[a] Determined by the stress between 0 and 10% strain.

Figure 26 Tensile strength of poly(*n*-butyl acrylate) (poly(BA))-based rotaxane crosslinked polymers (RCPs) and covalently crosslinked polymers (CCPs). (**a**) Stress–strain curves. (**b**) Summarized data of the tensile tests. A full colour version of this figure is available at the *Polymer Journal* journal online.

and star and linear structures, denoted **$Star_4$-Model** and **Linear-Model**, that were synthesized for comparison. The plots of **Rot-$Star_4$_A** and **$Star_4$-Model** as well as that of **Rot-Linear_U** and **Linear-Model** were relatively close but not overlapping, whereas the intrinsic viscosity of **Rot-$Star_4$_A** ($[\eta] = 0.18$) was lower than that of **Rot-Linear_U** ($[\eta] = 0.22$). The g' value, which is defined as the ratio of the intrinsic viscosity of the branched polymer to the linear polymer with the same molecular weight, is generally used to theoretically evaluate the extent of branching. The g' value of **Rot-$Star_4$_A** to **Rot-Linear_U** was calculated to be $g' = 0.82$, and this is higher than that of the model polymer ($g' = 0.74$) but lower than that of the rotaxane-linked 3-arm polymer composed of PVL ($g' = 0.89$).[81] In general, the smaller the g' value, the larger the number of arm chains with same molecular weight in the star polymer. Therefore, the results suggest the successful synthesis of the multi-armed star polymer **Rot-$Star_4$_A** as well as its structural transformation to a linear-like polymer (**Rot-Linear_U**) whose polymer-dangling wheel component may be partially located on the urethane linkage at the axle end.

Figure 23b shows the Huggins plots of **Rot-$Star_6$_A**, **Rot-$Star_3$_U** and **Linear-Model**. These plots are distinct from one another. The $[\eta]$ value of **Rot-$Star_6$_A** was the smallest, and the $[\eta]$ value of **Rot-$Star_3$_U** was in between those of **Rot-$Star_6$_A** and **Linear-Model**. Accordingly, the g' values of **Rot-$Star_6$_A** to **Linear-Model** and **Rot-$Star_3$_A** to **Linear-Model** were 0.58 and 0.66, respectively. Although the g' value of **Rot-$Star_6$_A** was relatively consistent with the reported data, the g' value of **Rot-$Star_3$_A** is lower than the reported data.[89–91] This result may be attributed to the strength or weakness of the interaction between the axle and wheel components. **Rot-$Star_6$_A** is constructed from the strong *sec*-ammonium/crown ether interaction that can fix the wheel component around the core, in keeping with the 6-arm star polymer structure. In contrast, **Rot-$Star_3$_U** was constructed from the relatively weak urethane/crown interaction at the end of the axle polymer chain that is not sufficiently strong to fix the wheel component at the end of the axle polymer chain to maintain the 3-arm star structure of the entire polymer. As a result, **Rot-$Star_3$_U** also has a partially branched structure.[56] However, the present dynamic structural change originating from the mechanical linkage is very interesting from the viewpoint of polymer rheology.[55,92]

MULTIPLEX LINKING DIRECTED TOWARD MOVABLE CROSSLINKS THROUGH ROTAXANE LINKAGE

The dynamic systems utilizing the mobile or switching function of rotaxane mentioned above can also be observed in rotaxane crosslinked polymers (RCPs) with rotaxane structures at the crosslink points and where the polymer chains are not fixed at the crosslink points. The interesting properties of RCPs, such as high swellability, stretchability and stress-relaxing function, mainly result from the high mobility of the polymer chains at the crosslink point. Such movable crosslinks are distinguished from typical physical and chemical crosslinks that have fixed crosslinked points.

The first synthesis of RCP was reported by the Gibson group in 1992.[65,66,93–96] They obtained gelled products via the polycondensation of a macrocycle-tethering monomer, that is, a 32-membered crown ether monomer. The occurrence of gelation is considered to result from the permanent physical entanglements arising from the threading of the polymer chain into the macrocycle cavity. The driving force is attributed to the attractive interaction of the crown ether wheel containing polyamide and polyurethane segments formed by the polycondensation. They also confirmed the presence of the rotaxane structure by nuclear magnetic resonance, whereby some nuclear Overhauser effect between the urethane linkage and the wheel was observed.

de Gennes[97] reported the theoretical prediction of the unique properties of RCP in 1999. Okumura and Ito[98] synthesized an RCP called a 'slide-ring gel' by covalently crosslinking the cyclodextrin moiety of polyrotaxane-containing cyclodextrin moieties as wheel components and PEO as an axle component. Furthermore, they revealed the prominent properties and wide applicability via the preparation of various slide-ring gels.[99–105] These pioneering works were followed by a variety of studies in which the movable junction point played a crucial role.[106–122]

In these reports on RCPs, the number of wheel components utilized for the crosslink points and their movable length or range on the axle

a

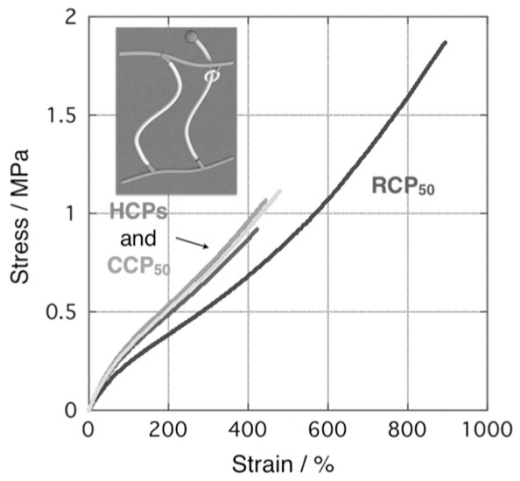

b

Entry	Cross-linked polymer	RC : CC	Fracture strain [%]	Fracture stress [MPa]
1	**RCP$_{50}$**	100 : 0	890	1.9
2	**HCP$_{75}$**	75 : 25	420	0.92
3	**HCP$_{50}$**	50 : 50	480	1.1
4	**HCP$_{25}$**	25 : 75	270	0.65
5	**CCP$_{50}$**	0 : 100	440	1.1

Figure 27 Tensile strength of poly(*n*-butyl acrylate) (poly(BA))-based hybrid crosslinked polymers (HCLPs) along with **RCP$_{50}$** and **CCP$_{50}$**. (**a**) Stress–strain curves. (**b**) Summary of the tensile tests. CCP, covalently crosslinked polymer; RCP, rotaxane crosslinked polymer. A full colour version of this figure is available at the *Polymer Journal* journal online.

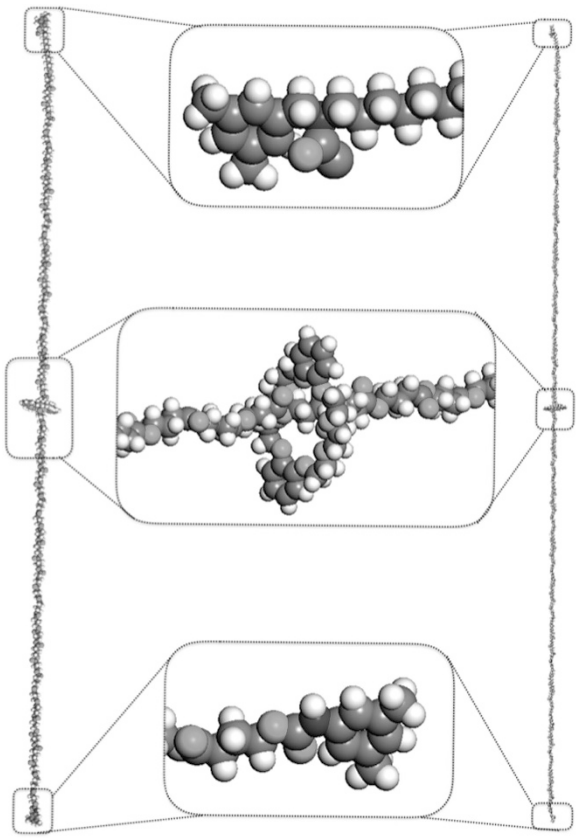

Figure 28 Simulated structures of two M2Rs ($n=25$ (left) and 50 (right), obtained using the OPLS2005 software MacroModel 9.9, New York, NY, USA). M2R, macromolecular [2]rotaxane. A full colour version of this figure is available at the *Polymer Journal* journal online.

polymer strongly relate to the physical properties of the RCP. However, essential studies of the relation between the structure of the rotaxane crosslinker (RC) and the physical properties of the corresponding RCP are rarely reported because the RCs reported so far do not have a defined structure but are complex. The complexity of RCs makes it difficult to evaluate how the axle length and wheel number of an RC affect the physical properties of the corresponding RCP. Because of such circumstances, we were inspired to develop an RC with a definite structure, containing two vinyl groups in the two components of M2R, and applied it to vinyl polymer systems.[123] The M2R-based RC is expected to be an ideal model to clarify the relation between the movable length of the wheel component or axle length for wheel movement and the properties of RCP (Figure 24).

An M2R-based RC containing a polymeric axle and a wheel component was synthesized for the first time using the method shown in Scheme 15.

To synthesize the M2R-based RC, we prepared an M2R containing a *sec*-ammonium salt with a terminal hydroxyl group and DB24C8 with a methacrylate group. According to Scheme 15, two M2Rs with different molecular weights were prepared via the living ring-opening polymerization of δ-VL via the rotaxane-from method, followed by the successive capping of the OH propagating end with a bulky isocyanate. Modification of the *sec*-ammonium moiety of the M2Rs with methacryloyloxyethyl isocyanate in tetrahydrofuran resulted in the formation of M2R-based RCs with high overall yields. Among the two RCs, **RC$_{25}$** contained PVL with a DP of 25 as the axle component, whereas **RC$_{50}$** contained PVL with a DP of 50. As a reference to RC, two covalent crosslinkers (CCs) with the same repeating units and DPs (**CC$_{25}$** and **CC$_{50}$**) were independently prepared for comparison (Scheme 15b). Table 2 summarizes the results of the synthesis of the RCs and CCs.

To further examine the effect of the crosslinkers, *n*-butyl acrylate (BA) and 2-ethylhexyl acrylate (EHA) were chosen as typical vinyl monomers because of the ease of evaluation of the elastic properties of their polymers, poly(BA) and poly(EHA), as the glass transition temperature (T_g) is below room temperature. The radical polymerizations of BA and EHA were conducted in the presence of 0.5 mol % RC and CC (Scheme 16). The ultraviolet irradiation of the mixture containing a photoinitiator for 5 min under ambient conditions afforded the corresponding RCPs and covalently crosslinked polymers (CCPs) as gel films. The RCPs were purified by swelling and washing with $CHCl_3$ and MeOH repeatedly to remove unreacted monomer and soluble materials. The RCPs and CCPs, as elastic polymers, had a T_g of ~ − 50 °C that was similar to that of the poly(BA) and poly(EHA) homopolymers.

The swelling ratios of the poly(BA)-based RCPs and CCPs toward chloroform are shown in Figure 25. The swelling ratios of the RCPs were higher than those of the CCPs, probably indicating the higher homogeneity of the network originating from the rotaxane crosslinks. Meanwhile, the degree of polymerization with respect to the length of the polymer chain had little effect on the swelling behavior.

Figure 26a shows the stress–strain curves of the RCPs and CCPs, and their mechanical properties data are summarized in Figure 26b. The toughness, that is, fracture stress and strain, of the RCPs was much larger than that of the CCPs. Interestingly, although a higher degree of polymerization of VL produced a higher Young's modulus (**CCP$_{50}$** > **CCP$_{25}$**) in CCP, whereby the PVL segment acts as the hard

segment, the RCPs showed the reverse behavior. Moreover, the fracture energy of the RCPs increased in proportion to the axle length of the RCs. The poly(EHA)-based RCPs had a similar tendency as the poly(BA)-based RCPs, suggesting that the relaxation effect of the movable linkage at the crosslink points on their properties is different from that of typical covalently crosslinked polymer.

To contrast the effects of RCs and CCs, 'hybrid' crosslinked polymers with both rotaxane crosslinks and covalent cross-links were synthesized using BA as a matrix monomer. The mechanical properties of the hybrid crosslinked polymers obtained using a total concentration of the crosslinkers of 0.5 mol% were evaluated (Figure 27). Interestingly, all hybrid crosslinked polymers showed similar behaviors to $\mathbf{CCP_{50}}$ independent of the feed ratio of RC and CC. This result seems reasonable because the crosslink points formed by CC produce a fragile point for fracture when stress is loaded before the rotaxane crosslink is formed. Thus, the present study strongly suggests the usefulness of rotaxane crosslinkers, that is, M2R-based RC, that can endow vinyl polymers with toughness in a simple manner. In addition, the M2R based-RC would strongly contribute to the clarification of the actual mechanism in the generation of toughness by the rotaxane crosslinks.

CONCLUSIONS AND OUTLOOK

In this review, we discussed the construction and function of dynamic macromolecular systems containing mechanically linked polymer chains that can undergo topology transformations to induce structural and property changes. The structure-definite polyrotaxane M2R containing one axle polymer chain and one wheel component played a crucial role in the fabrication of rotaxane-linked (block) polymers, topology-transformable polymers and rotaxane crosslinkers. The positional control of the crown ether wheel on the axle component by changing the degree of interaction with the axle polymer clearly correlated to the crystallization behavior of the axle polymer in M2R. Notably, the presence of only one wheel affected the crystallization behavior of M2R, even though the size of the wheel component was very small (Figure 28).

We first described the linear–cyclic polymer topology transformation by using [1]polyrotaxane to emphasize the role of the rotaxane linking of the polymer chain. Then, we discussed the synthesis of rotaxane-linked (co)polymers and their topology transformations. Control of the intercomponent interaction could produce a variety of novel dynamic polymer systems through polymer topology changes from linear to branched, star to linear and star to star that clearly caused property changes. Furthermore, a structure-definite RC with two vinyl groups in each M2R component was synthesized to prepare the corresponding RCP that showed excellent toughness compared with that of a CCP.

As present research into the construction of dynamic macromolecular systems utilizing rotaxane linkages only began several years ago, there are many problems to be solved. We are now focusing on the study of the effect of the component-relative position and mobility in the bulk state of M2R and its derivatives. Such fundamental studies will contribute to the effective tuning of the properties of M2R-based characteristic polymers. Thus, M2R has great potential to remarkably expand the fields of polymer and materials science.

CONFLICT OF INTEREST

The authors declare no conflict of interest.

1 Poelma, J. E., Ono, K., Miyajima, D., Aida, T., Satoh, K. & Hawker, C. J. Cyclic block copolymers for controlling feature sizes in block copolymer lithography. *ACS Nano* **6**, 10845–10854 (2012).
2 Lee, J. H., Driva, P., Hadjichristidis, N., Wright, P. J., Rucker, S. P. & Lohse, D. J. Damping behavior of entangled comb polymers: experiment. *Macromolecules* **42**, 1392–1399 (2009).
3 Aoshima, S. & Kanaoka, S. A renaissance in living cationic polymerization. *Chem. Rev.* **109**, 5245–5287 (2009).
4 Lee, J. H., Orfanou, K., Driva, P., Iatrou, H., Hadjichristidis, N. & Lohse, D. J. Linear and nonlinear rheology of dendritic star polymers: experiment. *Macromolecules* **41**, 9165–9178 (2008).
5 Aoshima, S., Yoshida, T., Kanazawa, A. & Kanaoka, S. New stage in living cationic polymerization: an array of effective Lewis acid catalysts and fast living polymerization in seconds. *J. Polym. Sci. A Polym. Chem.* **45**, 1801–1813 (2007).
6 Jia, Z. F., Chen, H., Zhu, X. Y. & Yan, D. Y. Backbone-thermoresponsive hyperbranched polyethers. *J. Am. Chem. Soc.* **128**, 8144–8145 (2006).
7 Grayson, S. M. & Frechet, J. M. J. Convergent dendrons and dendrimers: from synthesis to applications. *Chem. Rev.* **101**, 3819–3867 (2001).
8 Guan, Z. B., Cotts, P. M., McCord, E. F. & McLain, S. J. Chain walking: a new strategy to control polymer topology. *Science* **283**, 2059–2062 (1999).
9 Floudas, G., Pispas, S., Hadjichristidis, N., Pakula, T. & Erukhimovich, I. Microphase separation in star block copolymers of styrene and isoprene. Theory, experiment, and simulation. *Macromolecules* **29**, 4142–4154 (1996).
10 Deng, Y., Zhang, S., Lu, G. L. & Huang, X. Y. Constructing well-defined star graft copolymers. *Polym. Chem.* **4**, 1289–1299 (2013).
11 Liu, H. H., Li, S. X., Zhang, M. J., Shao, W. & Zhao, Y. L. Facile synthesis of ABCDE-type H-shaped quintopolymers by combination of ATRP, ROP, and click chemistry and their potential applications as drug carriers. *J. Polym. Sci. A Polym. Chem.* **50**, 4705–4716 (2012).
12 Laurent, B. A. & Grayson, S. M. Synthetic approaches for the preparation of cyclic polymers. *Chem. Soc. Rev.* **38**, 2202–2213 (2009).
13 Hoskins, J. N. & Grayson, S. M. Synthesis and degradation behavior of cyclic poly (epsilon-caprolactone). *Macromolecules* **42**, 6406–6413 (2009).
14 Honda, S., Yamamoto, T. & Tezuka, Y. Tuneable enhancement of the salt and thermal stability of polymeric micelles by cyclized amphiphiles. *Nat. Commun.* **4**, 1574–1579 (2013).
15 Hecht, S. & Frechet, J. M. J. Dendritic encapsulation of function: applying nature's site isolation principle from biomimetics to materials science. *Angew. Chem. Int. Ed.* **40**, 74–91 (2001).
16 Voit, B.I. & Lederer, A. Hyperbranched and highly branched polymer architectures-synthetic strategies and major characterization aspects. *Chem. Rev.* **109**, 5924–5973 (2009).
17 Igari, M., Heguri, H., Yamamoto, T. & Tezuka, Y. Folding construction of doubly fused tricyclic, beta- and gamma-graph polymer topologies with kyklo-telechelic precursors obtained through an orthogonal click/ESA-CF protocol. *Macromolecules* **46**, 7303–7315 (2013).
18 Castro-Osma, J. A., Alonso-Moreno, C., Garcia-Martinez, J. C., Fernandez-Baeza, J., Sanchez-Barba, L. F., Lara-Sanchez, A. & Otero, A. Ring-opening (ROP) versus ring-expansion (REP) polymerization of epsilon-caprolactone to give linear or cyclic polycaprolactones. *Macromolecules* **46**, 6388–6394 (2013).
19 Dong, B. T., Dong, Y. Q., Du, F. S. & Li, Z. C. Controlling polymer topology by atom transfer radical self-condensing vinyl polymerization of p-(2-bromoisobutyloylmethyl) styrene. *Macromolecules* **43**, 8790–8798 (2010).
20 Wan, H. S., Chen, Y., Chen, L., Zhu, X. Y., Yan, D. Y., Li, B., Liu, T., Zhao, L., Jiang, X. L. & Zhang, G. Z. Supramolecular control of the branched topology of poly(sulfone-amine) from divinylsulfone and hexamethylenediamine. *Macromolecules* **41**, 465–470 (2008).
21 Dietrich-Buchecker, C. O. & Sauvage, J. P. Interlocking of molecular threads - from the statistical approach to the templated synthesis of catenands. *Chem. Rev.* **87**, 795–810 (1987).
22 Amabilino, D. B. & Stoddart, J. F. Interlocked and intertwined structures and superstructures. *Chem. Rev.* **95**, 2725–2828 (1995).
23 Nepogodiev, S. A. & Stoddart, J. F. Cyclodextrin-based catenanes and rotaxanes. *Chem. Rev.* **98**, 1959–1976 (1998).
24 Raymo, F. M. & Stoddart, J. F. Interlocked macromolecules. *Chem. Rev.* **99**, 1643–1663 (1999).
25 Takata, T. Polyrotaxane and polyrotaxane network: supramolecular architectures based on the concept of dynamic covalent bond chemistry. *Polym. J.* **38**, 1–20 (2006).
26 Forgan, R. S., Sauvage, J. P. & Stoddart, J. F. Chemical topology: complex molecular knots, links, and entanglements. *Chem. Rev.* **111**, 5434–5464 (2011).
27 Erbas-Cakmak, S., Leigh, D. A., McTernan, C. T. & Nussbaumer, A. L. Artificial molecular machines. *Chem. Rev.* **115**, 10081–10206 (2015).
28 Harada, A., Hashidzume, A., Yamaguchi, H. & Takashima, Y. Polymeric rotaxanes. *Chem. Rev.* **109**, 5974–6023 (2009).
29 Gibson, H. W., Bheda, M. C. & Engen, P. T. Rotaxanes, catenanes, polyrotaxanes, polycatenanes and related materials. *Prog. Polym. Sci.* **19**, 843–945 (1994).
30 Huang, F. H. & Gibson, H. W. Polypseudorotaxanes and polyrotaxanes. *Prog. Polym. Sci.* **30**, 982–1018 (2005).
31 Arunachalam, M. & Gibson, H. W. Recent developments in polypseudorotaxanes and polyrotaxanes. *Prog. Polym. Sci.* **39**, 1043–1073 (2014).

32 Mogi, Y., Nomura, M., Kotsuji, H., Ohnishi, K., Matsushita, Y. & Noda, I. Superlattice structures in morphologies of the ABC triblock copolymers. *Macromolecules* **27**, 6755–6760 (1994).
33 Takano, A., Wada, S., Sato, S., Araki, T., Hirahara, K., Kazama, T., Kawahara, S., Isono, Y., Ohno, A., Tanaka, N. & Matsushita, Y. Observation of cylinder-based microphase-separated structures from ABC star-shaped terpolymers investigated by electron computerized tomography. *Macromolecules* **37**, 9941–9946 (2004).
34 De Bo, G., De Winter, J., Gerbaux, P. & Fustin, C. A. Rotaxane-based mechanically linked block copolymers. *Angew. Chem. Int. Ed.* **50**, 9093–9096 (2011).
35 Aoki, D., Uchida, S., Nakazono, K., Koyama, Y. & Takata, T. Macromolecular [2] rotaxanes: effective synthesis and characterization. *ACS Macro Lett.* **2**, 461–465 (2013).
36 Yamaguchi, N. & Gibson, H. W. Formation of supramolecular polymers from homoditopic molecules containing secondary ammonium ions and crown ether moieties. *Angew. Chem. Int. Ed.* **38**, 143–147 (1999).
37 Guidry, E. N., Li, J., Stoddart, J. F. & Grubbs, R. H. Bifunctional [c2]Daisy-chains and their incorporation into mechanically interlocked polymers. *J. Am. Chem. Soc.* **129**, 8944–8945 (2007).
38 Kolchinski, A. G., Busch, D. H. & Alcock, N. W. Gaining control over molecular threading-benefits of 2nd coordination sites and aqueous-organic interfaces in rotaxane synthesis. *J. Chem. Soc. Chem. Commun.* 1289–1291 (1995).
39 Dong, S. Y., Zheng, B., Xu, D. H., Yan, X. Z., Zhang, M. M. & Huang, F. H. A crown ether appended super gelator with multiple stimulus responsiveness. *Adv. Mater.* **24**, 3191–3195 (2012).
40 Caputo, C. B., Zhu, K. L., Vukotic, V. N., Loeb, S. J. & Stephan, D. W. Heterolytic activation of H2 using a mechanically interlocked molecule as a frustrated Lewis base. *Angew. Chem. Int. Ed.* **52**, 960–963 (2013).
41 Ashton, P. R., Campbell, P. J., Chrystal, E. J. T., Glink, P. T., Menzer, S., Philp, D., Spencer, N., Stoddart, J. F., Tasker, P. A. & Williams, D. J. Dialkylammonium ion crown-ether complexes - the forerunners of a new family of interlocked molecules. *Angew. Chem. Int. Edit.* **34**, 1865–1869 (1995).
42 Cantrill, S. J., Fulton, D. A., Fyfe, M. C. T., Stoddart, J. F., White, A. J. P. & Williams, D. J. A new protocol for rotaxane synthesis. *Tetrahedron Lett.* **40**, 3669–3672 (1999).
43 Dietrich-Buchecker, C. O., Sauvage, J. P. & Kintzinger, J. P. A new family of molecules - metallo-catenanes. *Tetrahedron Lett.* **24**, 5095–5098 (1983).
44 Dietrich-Buchecker, C. O., Sauvage, J. P. & Kern, J. M. Templated synthesis of interlocked macrocyclic ligands-the catenands. *J. Am. Chem. Soc.* **106**, 3043–3045 (1984).
45 Ahamed, B. N., Duchene, R., Robeyns, K. & Fustin, C. A. Catenane-based mechanically-linked block copolymers. *Chem. Commun.* **52**, 2149–2152 (2016).
46 Furusho, Y., Matsuyama, T., Takata, T., Moriuchi, T. & Hirao, T. Synthesis of novel interlocked systems utilizing a palladium complex with 2,6-pyridinedicarbox-amide-based tridentate macrocyclic ligand. *Tetrahedron Lett.* **45**, 9593–9597 (2004).
47 Miyagawa, N., Watanabe, M., Matsuyama, T., Koyama, Y., Moriuchi, T., Hirao, T., Furusho, Y. & Takata, T. Successive catalytic reactions specific to Pd-based rotaxane complexes as a result of wheel translation along the axle. *Chem. Commun.* **46**, 1920–1922 (2010).
48 Ogawa, M., Nagashima, M., Sogawa, H., Kuwata, S. & Takata, T. Synthesis and cavity size effect of Pd-containing macrocycle catalyst for efficient intramolecular hydro-amination of allylurethane. *Org. Lett.* **17**, 1664–1667 (2015).
49 Beves, J. E., Blight, B. A., Campbell, C. J., Leigh, D. A. & McBurney, R. T. Strategies and tactics for the metal-directed synthesis of rotaxanes, knots, catenanes, and higher order links. *Angew. Chem. Int. Ed.* **50**, 9260–9327 (2011).
50 Ashton, P. R., Chrystal, E. J. T., Glink, P. T., Menzer, S., Schiavo, C., Spencer, N., Stoddart, J. F., Tasker, P. A., White, A. J. P. & Williams, D. J. Pseudorotaxanes formed between secondary dialkylammonium salts and crown ethers. *Chem. Eur. J.* **2**, 709–728 (1996).
51 Takata, T. & Kihara, N. Rotaxanes synthesized from crown ethers and sec-ammonium salts. *Rev. Heteroatom. Chem.* **22**, 197–218 (2000).
52 Nakazono, K. & Takata, T. Neutralization of a sec-ammonium group unusually stabilized by the "rotaxane effect": synthesis, structure, and dynamic nature of a "free" sec-amine/crown ether-type rotaxane. *Chem. Eur. J.* **16**, 13783–13794 (2010).
53 Suzuki, S., Nakazono, K. & Takata, T. Selective transformation of a crown ether/sec-ammonium salt-type rotaxane to N-alkylated rotaxanes. *Org. Lett.* **12**, 712–715 (2010).
54 Makiguchi, K., Satoh, T. & Kakuchi, T. Diphenyl phosphate as an efficient cationic organocatalyst for controlled/living ring-opening polymerization of delta-valerolactone and epsilon-caprolactone. *Macromolecules* **44**, 1999–2005 (2011).
55 Chen, Z., Aoki, D., Uchida, S., Marubayashi, H., Nojima, S. & Takata, T. Effect of component mobility on the properties of macromolecular [2] rotaxanes. *Angew. Chem. Int. Ed.* **55**, 2778–2781 (2016).
56 Ogawa, T., Nakazono, K., Aoki, D., Uchida, S. & Takata, T. Effective approach to cyclic polymer from linear polymer: synthesis and transformation of macromolecular [1]rotaxane. *ACS Macro Lett.* **4**, 343–347 (2015).
57 Ogawa, T., Usuki, N., Nakazono, K., Koyama, Y. & Takata, T. Linear-cyclic polymer structural transformation and its reversible control using a rational rotaxane strategy. *Chem. Commun.* **51**, 5606–5609 (2015).
58 Valentina, S., Ogawa, T., Nakazono, K., Aoki, D. & Takata, T. Efficient synthesis of cyclic block copolymers by rotaxane protocol by linear/cyclic topology transformation. *Chem. Eur. J.* **22**, 8759–8762 (2016).
59 Tezuka, Y. Topological polymer chemistry for designing multicyclic macromolecular architectures. *Polym. J.* **44**, 1159–1169 (2012).
60 Yamamoto, T. & Tezuka, Y. Cyclic polymers revealing topology effects upon self-assemblies, dynamics and responses. *Soft Matter* **11**, 7458–7468 (2015).
61 Aoki, D., Uchida, S. & Takata, T. Mechanically linked block/graft copolymers: effective synthesis via functional macromolecular [2]rotaxanes. *ACS Macro Lett.* **3**, 324–328 (2014).
62 Aoki, D., Uchida, S. & Takata, T. Synthesis and characterization of a mechanically linked transformable polymer. *Polym. J.* **46**, 546–552 (2014).
63 Gong, C. G. & Gibson, H. W. Synthesis and characterization of a polyester/crown ether rotaxane derived from a difunctional blocking group. *Macromolecules* **29**, 7029–7033 (1996).
64 Gibson, H. W., Liu, S., Gong, C. G., Ji, Q. & Joseph, E. Studies of the formation of poly (ester rotaxane)s from diacid chlorides, diols, and crown ethers and their properties. *Macromolecules* **30**, 3711–3727 (1997).
65 Gong, C. G. & Gibson, H. W. Controlling polymeric topology by polymerization conditions: Mechanically linked network and branched poly(urethane rotaxane)s with controllable polydispersity. *J. Am. Chem. Soc.* **119**, 8585–8591 (1997).
66 Gong, C. G. & Gibson, H. W. Self-threading-based approach for branched and/or cross-linked poly(methacrylate rotaxane)s. *J. Am. Chem. Soc.* **119**, 5862–5866 (1997).
67 Kobatake, S., Takami, S., Muto, H., Ishikawa, T. & Irie, M. Rapid and reversible shape changes of molecular crystals on photoirradiation. *Nature* **446**, 778–781 (2007).
68 Fang, L., Hmadeh, M., Wu, J. S., Olson, M. A., Spruell, J. M., Trabolsi, A., Yang, Y. W., Elhabiri, M., Albrecht-Gary, A. M. & Stoddart, J. F. Acid-base actuation of [c2] daisy chains. *J. Am. Chem. Soc.* **131**, 7126–7134 (2009).
69 Romuald, C., Arda, A., Clavel, C., Jimenez-Barbero, J. & Coutrot, F. Tightening or loosening a pH-sensitive double-lasso molecular machine readily synthesized from an ends-activated [c2]daisy chain. *Chem. Sci.* **3**, 1851–1857 (2012).
70 Yuan, C. X., Saito, S., Camacho, C., Irle, S., Hisaki, I. & Yamaguchi, S. A pi-conjugated system with flexibility and rigidity that shows environment-dependent RGB luminescence. *J. Am. Chem. Soc.* **135**, 8842–8845 (2013).
71 Hadjichristidis, N., Pitsikalis, M., Pispas, S. & Iatrou, H. Polymers with complex architecture by living anionic polymerization. *Chem. Rev.* **101**, 3747–3792 (2001).
72 Ouchi, M., Terashima, T. & Sawamoto, M. Transition metal-catalyzed living radical polymerization: toward perfection in catalysis and precision polymer synthesis. *Chem. Rev.* **109**, 4963–5050 (2009).
73 Ren, J. M., McKenzie, T. G., Fu, Q., Wong, E. H. H., Xu, J. T., An, Z. S., Shanmugam, S., Davis, T. P., Boyer, C. & Qiao, G. G. Star polymers. *Chem. Rev.* **116**, 6743–6836 (2016).
74 Mignani, S., El Kazzouli, S., Bousmina, M. M. & Majoral, J. P. Dendrimer space exploration: an assessment of dendrimers/dendritic scaffolding as inhibitors of protein-protein interactions, a potential new area of pharmaceutical development. *Chem. Rev.* **114**, 1327–1342 (2014).
75 Bosman, A. W., Janssen, H. M. & Meijer, E. W. About dendrimers: structure, physical properties, and applications. *Chem. Rev.* **99**, 1665–1688 (1999).
76 Villaraza, A. J. L., Bumb, A. & Brechbiel, M. W. Macromolecules, dendrimers, and nanomaterials in magnetic resonance imaging: the interplay between size, function, and pharmacokinetics. *Chem. Rev.* **110**, 2921–2959 (2010).
77 Altintas, O., Gerstel, P., Dingenouts, N. & Barner-Kowollik, C. Single chain self-assembly: preparation of alpha,omega-donor-acceptor chains via living radical polymerization and orthogonal conjugation. *Chem. Commun.* **46**, 6291–6293 (2010).
78 Schappacher, M. & Deffieux, A. Reversible switching between linear and ring polystyrenes bearing porphyrin end groups. *J. Am. Chem. Soc.* **133**, 1630–1633 (2011).
79 Zhao, Y., Tremblay, L. & Zhao, Y. Phototunable LCST of water-soluble polymers: exploring a topological effect. *Macromolecules* **44**, 4007–4011 (2011).
80 Yamamoto, T., Yagyu, S. & Tezuka, Y. Light- and heat-triggered reversible linear-cyclic topological conversion of telechelic polymers with anthryl end groups. *J. Am. Chem. Soc.* **138**, 3904–3911 (2016).
81 Aoki, D., Uchida, S. & Takata, T. Star/linear polymer topology transformation facilitated by mechanical linking of polymer chains. *Angew. Chem. Int. Ed.* **54**, 6770–6774 (2015).
82 Sato, H., Aoki, D. & Takata, T. Synthesis and star/linear topology transformation of a mechanically linked ABC terpolymer. *ACS Macro Lett* **5**, 699–703 (2016).
83 Hirose, T., Aoki, D., Monjiyama, S., Sogawa, H., Uchida, S. & Takata, T. Synthesis of star polymers having changeable arm number and length facilitated by mechanical linkage. (to be submitted).
84 Koyama, Y., Miura, K., Cheawchan, S., Seo, A. & Takata, T. Cascade functionalization of unsaturated bond-containing polymers using ambident agents possessing both nitrile N-oxide and electrophilic functions. *Chem. Commun. (Camb)* **48**, 10304–10306 (2012).
85 Cheawchan, S., Koyama, Y., Uchida, S. & Takata, T. Catalyst-free click cascade functionalization of unsaturated-bond-containing polymers using masked-ketene-tethering nitrile N-oxide. *Polymer* **54**, 4501–4510 (2013).
86 Cheawchan, S., Uchida, S., Sogawa, H., Koyama, Y. & Takata, T. Thermotriggered catalyst-free modification of a glass surface with an orthogonal agent possessing nitrile N-oxide and masked ketene functions. *Langmuir* **32**, 309–315 (2016).

87 Wang, C. G., Koyama, Y., Yonekawa, M., Uchida, S. & Takata, T. Polymer nitrile N-oxides directed toward catalyst- and solvent-free click grafting. *Chem. Commun.* **49**, 7723–7725 (2013).
88 Wang, C. G., Koyama, Y., Uchida, S. & Takata, T. Synthesis of highly reactive polymer nitrile N-oxides for effective solvent-free grafting. *ACS Macro Lett.* **3**, 286–290 (2014).
89 Sanda, F., Sanada, H., Shibasaki, Y. & Endo, T. Star polymer synthesis from epsilon-caprolactone utilizing polyol/protonic acid initiator. *Macromolecules* **35**, 680–683 (2002).
90 Graessley, W. W. & Roovers, J. Melt rheology of 4-arm and 6-arm star polystyrenes. *Macromolecules* **12**, 959–965 (1979).
91 Roovers, J. Synthesis and dilute-solution characterization of comb polystyrenes. *Polymer* **20**, 843–849 (1979).
92 Kohsaka, Y., Koyama, Y. & Takata, T. Graft polyrotaxanes: a new class of graft copolymers with mobile graft chains. *Angew. Chem. Int. Ed.* **50**, 10417 (2011).
93 Delaviz, Y. & Gibson, H. W. Macrocyclic polymers. 2. Synthesis of poly(amide crown ethers) based on bis(5-carboxy-1,3-phenylene)-32-crown-10. Network formation through threading. *Macromolecules* **25**, 4859–4862 (1992).
94 Delaviz, Y. & Gibson, H. W. Macrocyclic polymers. 1. Synthesis of a poly(ester crown) based on bis(5-carboxy-1,3-phenylene)-32-crown-10 and 4,4'-isopropylidenediphenol (bisphenol-A). *Macromolecules* **25**, 18–20 (1992).
95 Gibson, H. W., Nagvekar, D. S., Powell, J., Gong, C. G. & Bryant, W. S. Polyrotaxanes by in situ self threading during polymerization of functional macrocycles. 2. Poly(ester crown ether)s. *Tetrahedron* **53**, 15197–15207 (1997).
96 Gong, C. G. & Gibson, H. W. Supramolecular chemistry with macromolecules: macromolecular knitting, reversible formation of branched polyrotaxanes by self-assembly. *Macromol. Chem. Phys.* **199**, 1801–1806 (1998).
97 de Gennes, P. G. Sliding gels. *Physica A* **271**, 231–237 (1999).
98 Okumura, Y. & Ito, K. The polyrotaxane gel: a topological gel by figure-of-eight cross-links. *Adv. Mater.* **13**, 485–487 (2001).
99 Araki, J. & Ito, K. Recent advances in the preparation of cyclodextrin-based polyrotaxanes and their applications to soft materials. *Soft Matter* **3**, 1456–1473 (2007).
100 Bin Imran, A., Seki, T., Kataoka, T., Kidowaki, M., Ito, K. & Takeoka, Y. Fabrication of mechanically improved hydrogels using a movable cross-linker based on vinyl modified polyrotaxane. *Chem. Commun.* 5227–5229 (2008).
101 Bin Imran, A., Seki, T., Ito, K. & Takeoka, Y. Poly(N-isopropylacrylamide) gel prepared using a hydrophilic polyrotaxane-based movable cross-linker. *Macromolecules* **43**, 1975–1980 (2010).
102 Bin Imran, A., Esaki, K., Gotoh, H., Seki, T., Ito, K., Sakai, Y. & Takeoka, Y. Extremely stretchable thermosensitive hydrogels by introducing slide-ring polyrotaxane cross-linkers and ionic groups into the polymer network. *Nat. Commun.* **5**, 5124 (2014).
103 Kato, K., Yasuda, T. & Ito, K. Peculiar elasticity and strain hardening attributable to counteracting entropy of chain and ring in slide-ring gels. *Polymer* **55**, 2614–2619 (2014).
104 Li, X., Kang, H. L., Shen, J. X., Zhang, L. Q., Nishi, T., Ito, K., Zhao, C. M. & Coates, P. Highly toughened polylactide with novel sliding graft copolymer by in situ reactive compatibilization, crosslinking and chain extension. *Polymer* **55**, 4313–4323 (2014).
105 Uenuma, S., Maeda, R., Takahashi, S., Kato, K., Yokoyama, H. & Ito, K. Self-assembled structure of polyrotaxane consisting of beta-cyclodextrin and poly(ethylene oxide)-block-poly(propylene oxide)-block-poly(ethylene oxide) triblock copolymer in bulk system. *Chem. Lett.* **45**, 991–993 (2016).
106 Kihara, N., Hinoue, K. & Takata, T. Solid-state end-capping of pseudopolyrotaxane possessing hydroxy-terminated axle to polyrotaxane and its application to the synthesis of a functionalized polyrotaxane capable of yielding a polyrotaxane network. *Macromolecules* **38**, 223–226 (2005).
107 Oku, T., Furusho, Y. & Takata, T. A concept for recyclable cross-linked polymers: topologically networked polyrotaxane capable of undergoing reversible assembly and disassembly. *Angew. Chem. Int. Ed.* **43**, 966–969 (2004).
108 Tan, S., Blencowe, A., Ladewig, K. & Qiao, G. G. A novel one-pot approach towards dynamically cross-linked hydrogels. *Soft Matter* **9**, 5239–5250 (2013).
109 Cai, T., Yang, W. J., Zhang, Z. B., Zhu, X. L., Neoh, K. G. & Kang, E. T. Preparation of stimuli-responsive hydrogel networks with threaded beta-cyclodextrin end-capped chains via combination of controlled radical polymerization and click chemistry. *Soft Matter* **8**, 5612–5620 (2012).
110 Murakami, T., Schmidt, B. V. K. J., Brown, H. R. & Hawker, C. J. One-pot "click" fabrication of slide-ring gels. *Macromolecules* **48**, 7774–7781 (2015).
111 Bilig, T., Oku, T., Furusho, Y., Koyama, Y., Asai, S. & Takata, T. Polyrotaxane networks formed via rotaxanation utilizing dynamic covalent chemistry of disulfide. *Macromolecules* **41**, 8496–8503 (2008).
112 Kohsaka, Y., Nakazono, K., Koyama, Y., Asai, S. & Takata, T. Size-complementary rotaxane cross-linking for the stabilization and degradation of a supramolecular network. *Angew. Chem. Int. Ed.* **50**, 4872–4875 (2011).
113 Koyama, Y., Yoshii, T., Kohsaka, Y. & Takata, T. Photodegradable cross-linked polymer derived from a vinylic rotaxane cross-linker possessing aromatic disulfide axle. *Pure. Appl. Chem.* **85**, 835–842 (2013).
114 Ichi, T., Watanabe, J., Ooya, T. & Yui, N. Controllable erosion time and profile in poly (ethylene glycol) hydrogels by supramolecular structure of hydrolyzable polyrotaxane. *Biomacromolecules* **2**, 204–210 (2001).
115 Iijima, K., Aoki, D., Sogawa, H., Asai, S. & Takata, T. Synthesis and characterization of supramolecular cross-linkers containing cyclodextrin dimer and trimer. *Polym. Chem.* **7**, 3492–3495 (2016).
116 Kubo, M., Hibino, T., Tamura, M., Uno, T. & Itoh, T. Synthesis and copolymerization of cyclic macromonomer based on cyclic polystyrene: gel formation via chain threading. *Macromolecules* **35**, 5816–5820 (2002).
117 Ogawa, M., Kawasaki, A., Koyama, Y. & Takata, T. Synthesis and properties of a polyrotaxane network prepared from a Pd-templated bis-macrocycle as a topological cross-linker. *Polym. J.* **43**, 909–915 (2011).
118 Oike, H., Mouri, T. & Tezuka, Y. A cyclic macromonomer designed for a novel polymer network architecture having both covalent and physical linkages. *Macromolecules* **34**, 6229–6234 (2001).
119 Zada, A., Avny, Y. & Zilkha, A. Monomers for non-bond crosslinking of vinyl polymers. *Eur. Polym. J.* **35**, 1159–1164 (1999).
120 Suzaki, Y., Taira, T. & Osakada, K. Physical gels based on supramolecular gelators, including host-guest complexes and pseudorotaxanes. *J. Mater. Chem.* **21**, 930–938 (2011).
121 Nakahata, M., Takashima, Y. & Harada, A. Supramolecular polymeric materials containing cyclodextrins. *Chem. Pharm. Bull.* **65**, 330–335 (2017).
122 Takashima, Y., Sawa, Y., Iwaso, K., Nakahata, M., Yamaguchi, H. & Harada, A. Supramolecular materials cross-linked by host-guest inclusion complexes: the effect of side chain molecules on mechanical properties. *Macromolecules* **50**, 3254–3261 (2017).
123 Sawada, J., Aoki, D., Uchida, S., Otsuka, H. & Takata, T. Synthesis of vinylic macromolecular rotaxane cross-linkers endowing network polymers with toughness. *ACS Macro Lett.* **4**, 598–601 (2015).

Toshikazu Takata is a professor of chemistry at Tokyo Institute of Technology (Tokyo Tech). He received his BS from Okayama University (1976), and PhD from Tsukuba University (1981) under the supervision of the late Professor Shigeru Oae. He moved to Tokyo Institute of Technology as an assistant professor in 1985 after spending few years as a research associate at Tsukuba University since 1981. He promoted to a full professor of Japan Advanced Institute of Science and Technology (JAIST) in 1994, after serving as an associate professor of Tokyo Tech from 1988. He moved to Osaka Prefecture University in 1995 and then Tokyo Tech in 2003. His research interest is to develop dynamic molecular and macromolecular systems with unique property and function using a supramolecular protocol in organic and polymer chemistry fields.

Daisuke Aoki is currently an assistant professor of Department of Chemical Science and Engineering at Tokyo Institute of Technology. He was born in Gunma Prefecture, Japan in 1983. He earned a BE and a ME in Polymer Engineering at Yamagata University, under the supervision of Professor O Haba. He obtained his PhD from the Tokyo Institute of Technology in 2014 under the supervision of Professor T Takata, working on polymer topological changes based on rotaxane structure. His research is focused on the synthesis and characterization of functional polymers with applications in material science.